Vibrational Spectroscopy 58 (2012) 169–180

Contents lists available at SciVerse ScienceDirect

Vibrational Spectroscopy

journal homepage: www.elsevier.com/locate/vibspec

Structural, calorimetric and vibrational investigations of 2, 3 and 4-hydroxyanilinium perchlorate: A theoretical and experimental study

Y. Erdogdu[a], M. Drozd[b], M.K. Marchewka[b,*]

[a] Department of Physics, Ahi Evran University, 40040 Kirsehir, Turkey
[b] Institute of Low Temperature and Structure Research, Polish Academy of Sciences, 50-950 Wrocław 2, Poland

ARTICLE INFO

Article history:
Received 2 September 2011
Received in revised form 31 October 2011
Accepted 1 December 2011
Available online 8 December 2011

Keywords:
Perchlorates
2-Hydroxyaniline
3-Hydroxyaniline
4-Hydroxyaniline
Hydrogen bonding
Differential scanning calorimetry
Phase transitions
FT-IR spectroscopy
Structure–spectra correlation
Second harmonic generation (SHG)

ABSTRACT

Complexes of perchloric acid with interesting physical properties are investigated in details. Single crystals of 2-hydroxyanilinium perchlorate (abbreviated as 2HAP-ClO_4), 3-hydroxyanilinium perchlorate (abbreviated as 3HAP-ClO_4), and 4-hydroxyanilinium perchlorate (abbreviated as 4HAP-ClO_4) were grown by the slow evaporation technique and vibrational spectral analysis was carried out using Far-IR and Fourier transform IR spectroscopy. The density functional theoretical (DFT) computations were also performed at the B3LYP/6-311++G(d,p) level to derive the equilibrium geometry, vibrational wavenumbers and intensities. The detailed interpretation of the vibrational spectra has been carried out with the aid of normal coordinate analysis (NCA) following the scaled quantum mechanical force field methodology.

1. Introduction

We paid our attention on perchloric acid because this acid forms interesting complexes with organic cations [1]. Some complexes of perchloric acid exhibit such nonlinear optical properties as second harmonic generation (SHG). The example is L-arginine perchlorate [2,3]. Second harmonic generation was also found for complexes of guanidine and L-leucine with perchloric acid [4]. The perchlorate anion was the subject of crystallographic studies [5]. There are many examples of perchlorates exhibiting structural phase transitions connected with the ordering of perchlorate anions. Such phenomenon was observed in solid trimethylammonium perchlorate by Stammler et al. [6]. Mylrajan [7] studied molecular motions in tetragonal tetramethylammonium perchlorate with the help of vibrational spectroscopy. Pyridinium perchlorate reveals two structural phase transitions at 233 and 345 K, the second one being of ferroelectric type [8,9]. P–T phase diagram of this compound was studied by Czarnecki et al. [10].

Among crystals comprising perchlorate anions, the most interesting for us are non-centrosymmetric because of the non-linear optical properties. For example, the pronounced second harmonic generation was found in L-leucinium perchlorate (SHG efficiency $d = 0.44d_{KDP}$), anilinium perchlorate (SHG efficiency $d = 0.20d_{KDP}$) and 4-nitroanilinum perchlorate [11]. Such results depend on noncentrosymmetric crystal structures of these crystals. Systems containing perchlorate anions exhibit structural phase transitions due to disorder of oxygen atoms. Such systems were intensively studied crystallographically [5] and spectroscopically [12]. Phase transitions were discovered for three crystalline complexes of melamine, L-leucine and L-arginine [4]. Perchlorate anions were the subject of investigations not only in condensed phase. Quite recently, Ji et al. [13], studied large angular jump mechanism observed for hydrogen bond exchange in aqueous perchlorate solution. Such studies are extremely important, as the detailed mechanism for H-bond switching in aqueous solution remains uncertain.

In the present work, we report the results of X-ray, theoretical and experimental vibrational spectra, differential scanning calorimetry (DSC), molecular orbital energies and molecular electrostatic potential (MESP) of 2, 3 and 4-hydroxyanilinium perchlorate compounds. The electronic and spectroscopic properties, phase transition of these have not yet been studied in detail

---

* Corresponding author. Tel.: +48 71 3954299; fax: +48 71 3441029.
E-mail addresses: yusuferdogdu@gmail.com (Y. Erdogdu), m.drozd@int.pan.wroc.pl (M. Drozd), m.marchewka@int.pan.wroc.pl, mkm@int.pan.wroc.pl (M.K. Marchewka).

0924-2031/$ – see front matter © 2011 Elsevier B.V. All rights reserved.
doi:10.1016/j.vibspec.2011.12.001

Table 1
The chain patterns of hydrogen bonds and the symmetry operation in the crystal structure of 2-, 3- and 4-hydroxyanilinium perchlorate (2HAP-ClO_4, 3HAP-ClO_4, 4HAP-ClO_4).

Descriptor of a pattern	Form	Symmetry operation	Position in the unit cell
2HAP-ClO_4			
$C^2_2(6)$	Left-handed helix ⊥ *b*	*c* (glide plane)	*x*, ½, *z*
$C^2_2(9)$	Left-handed helix ‖ *b*	2_1	¼, *y*, ¼
3HAP-ClO_4			
C(6)	Left-handed helix ‖ *b*	2_1	½, *y*, ½
$C^2_2(6)$	Simple chain	Translation along *b*	
$C^2_2(10)$	Simple chain	Translation along *c*	
$C^2_2(10)$	Simple chain	Translation along $[0\ 1\ \bar{1}]$	
4HAP-ClO_4			
$C^2_2(6)$	Simple chain	Translation along *a*	
$C^2_2(6)$	Left-handed helix ‖ *a*	2_1	*x*, ½, 0
$C^2_2(6)$	Right-handed helix ‖ *a*	2_1	*x*, ½, 0
$C^1_2(9)$	Right-handed helix ‖ *b*	2_1	0, *y*, ¼
$C^2_2(11)$	Left-handed helix ‖ *b*	2_1	½, *y*, ¼
$C^2_2(11)$	Right-handed helix ‖ *c*	2_1	¼, 0, *z*

to the best of our knowledge. Therefore, the present investigation was undertaken to study the molecular structure, vibrational spectra and phase transition of these compounds completely. Density Functional Theory (DFT/B3LYP) calculations have been performed to support our wavenumber assignments. Furthermore, we interpreted the calculated spectra in terms of total energy distributions (TED's) and made the assignment of the experimental bands.

2. Experimental

2.1. Preparation

The starting compounds, 2-hydroxyaniline (Aldrich, 99%), 3-hydroxyaniline (Aldrich, 98%), 4-hydroxyaniline (Aldrich, ≥98%) and perchloric acid (Aldrich, 70%), were used as supplied and prepared in the ratio of 1:1. The dissolved acid was added to the hot solution of 2-hydroxyaniline, 3-hydroxyaniline and 4-hydroxyaniline with the help of dropper. After the solution was cooled to room temperature, it remained clear, without any precipitants. Then, the solution was purified with the aid of active charcoal. The solution slowly evaporated during a few days till the crystals appeared.

2.2. Spectroscopic measurements

The vibrational measurements were carried out at room temperature. Infrared spectra were taken with a Bruker IFS-88 spectrometer in the region 4000–80 cm^{-1} with resolution 2 cm^{-1}. The polycrystalline powders were achieved by grinding in agate mortar with pestle. Samples, as suspensions in oil, were put between KBr wafers. The powder infrared spectra were taken in Nujol and Fluorolube emulsions to eliminate the bands originating from used oils. Far-infrared spectra in the 550–50 cm^{-1} region were measured in Nujol suspension between polyethylene plates. The measured spectra are shown on figures. The wavenumbers of the bands and their relative intensities are provided in tables. Bands revealed in this region were added to tables.

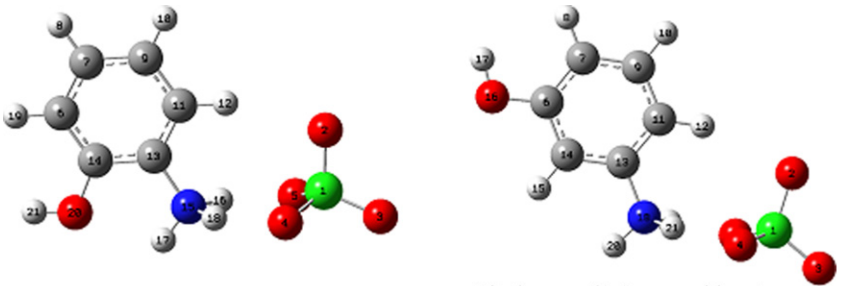

2-hydroxyanilinium perchlorate **3-hydroxyanilinium perchlorate**

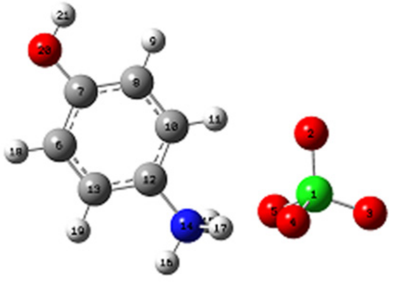

4-hydroxyanilinium perchlorate

Fig. 1. Optimized molecular structure and atomic numbering of 2, 3, 4 hydroxyanilinium perchlorate.

Table 2
Optimized geometric parameters of 2, 3 and 4-hydroxyanilinium perchlorate.

Bond lengths	4-Hydroxyaniline-$HClO_4$		Bond lengths	3-Hydroxyaniline-$HClO_4$		Bond lengths	2-Hydroxyaniline-$HClO_4$	
	B3LYP	X-ray		B3LYP	X-ray		B3LYP	X-ray
Cl_1-O_2	1.484		Cl_1-O_2	1.481	1.417	Cl_1-O_2	1.484	1.433
Cl_1-O_3	1.463		Cl_1-O_3	1.463	1.434	Cl_1-O_3	1.464	1.413
Cl_1-O_4	1.528		Cl_1-O_4	1.530	1.418	Cl_1-O_4	1.528	1.427
Cl_1-O_5	1.529		Cl_1-O_5	1.530	1.435	Cl_1-O_5	1.528	1.432
O_4-H_{17}	1.776		O_4-H_{21}	1.772		O_4-H_{18}	1.770	
O_5-H_{15}	1.765		O_5-H_{19}	1.752		O_5-H_{16}	1.774	
C_6-C_7	1.396	1.353	C_6-C_7	1.395	1.386	C_6-C_7	1.393	1.380
C_6-C_{13}	1.389	1.383	C_6-C_{14}	1.397	1.376	C_6-C_{14}	1.392	1.374
C_6-H_{18}	1.082	0.931	C_6-O_{16}	1.361	1.357	C_6-H_{19}	1.085	0.930
C_7-C_8	1.397	1.368	C_7-H_8	1.085	0.930	C_7-H_8	1.083	0.930
C_7-20	1.361	1.377	C_7-C_9	1.392	1.370	C_7-C_9	1.393	1.384
C_8-H_9	1.085	0.930	C_9-H_{10}	1.083	0.930	C_9-H_{10}	1.082	0.930
C_8-C_{10}	1.390	1.371	C_9-C_{11}	1.392	1.371	C_9-C_{11}	1.393	1.380
$C_{10}-H_{11}$	1.085	0.931	$C_{11}-H_{12}$	1.084	0.930	$C_{11}-H_{12}$	1.085	0.930
$C_{10}-C_{12}$	1.390	1.368	$C_{11}-C_{13}$	1.390	1.370	$C_{11}-C_{13}$	1.388	1.373
$C_{12}-C_{13}$	1.390	1.356	$C_{13}-C_{14}$	1.386	1.372	$C_{13}-C_{14}$	1.394	1.383
$C_{12}-N_{14}$	1.469	1.464	$C_{13}-N_{18}$	1.468	1.460	$C_{13}-N_{15}$	1.464	1.471
$C_{13}-H_{19}$	1.085	0.930	$C_{14}-H_{15}$	1.084	0.930	$C_{14}-O_{20}$	1.371	1.365
$N_{14}-H_{15}$	1.051	0.890	$O_{16}-H_{17}$	0.963	0.883	$N_{15}-H_{16}$	1.050	0.890
$N_{14}-H_{16}$	1.018	0.890	$N_{18}-H_{19}$	1.053	0.890	$N_{15}-H_{17}$	1.021	0.890
$N_{14}-H_{17}$	1.050	0.891	$N_{18}-H_{20}$	1.018	0.890	$N_{15}-H_{18}$	1.050	0.890
$O_{20}-H_{21}$	0.963	0.819	$N_{18}-H_{21}$	1.053	0.890	$O_{20}-H_{21}$	0.962	0.820

Bond angles	4-Hydroxyaniline-$HClO_4$		Bond angles	3-Hydroxyaniline-$HClO_4$		Bond angles	2-Hydroxyaniline-$HClO_4$	
	B3LYP	X-ray		B3LYP	X-ray		B3LYP	X-ray
$O_2-Cl_1-O_3$	112.6		$O_2-Cl_1-O_3$	112.7		$O_2-Cl_1-O_3$	112.6	109.9
$O_2-Cl_1-O_4$	108.6		$O_2-Cl_1-O_4$	108.7		$O_2-Cl_1-O_4$	108.6	109.5
$O_2-Cl_1-O_5$	108.6		$O_2-Cl_1-O_5$	108.7		$O_2-Cl_1-O_5$	108.6	107.5
$O_3-Cl_1-O_4$	110.3		$O_3-Cl_1-O_4$	110.1		$O_3-Cl_1-O_4$	110.2	110.7
$O_3-Cl_1-O_5$	110.2		$O_3-Cl_1-O_5$	110.1		$O_3-Cl_1-O_5$	110.2	110.5
$O_4-Cl_1-O_5$	105.9		$O_4-Cl_1-O_5$	105.8		$O_4-Cl_1-O_5$	106.0	107.5
$Cl_1-O_4-H_{17}$	108.5		$Cl_1-O_4-H_{12}$	73.68		$Cl_1-O_4-H_{18}$	108.5	
$Cl_1-O_5-H_{15}$	108.4		$Cl_1-O_5-H_{19}$	108.8		$Cl_1-O_5-H_{16}$	108.5	
$C_7-C_6-C_{13}$	119.6	119.8	$C_7-C_6-C_{14}$	119.9	120.4	$C_7-C_6-C_{14}$	119.4	120.2
$C_7-C_6-H_{18}$	119.2	120.8	$C_7-C_6-O_{16}$	123.3	123.4	$C_7-C_6-H_{19}$	120.6	119.8
$C_{13}-C_6-H_{18}$	121.0	120.0	$C_{14}-C_6-O_{16}$	116.7	117.0	$C_{14}-C_6-H_{19}$	119.9	119.9
$C_6-C_7-C_8$	120.0	120.2	$C_6-C_7-H_8$	119.9	119.8	$C_6-C_7-H_8$	119.2	119.8
$C_6-C_7-O_{20}$	117.1	118.0	$C_6-C_7-C_9$	119.8	120.2	$C_6-C_7-C_9$	120.7	120.3
$C_8-C_7-O_{20}$	122.8	121.7	$H_8-C_7-C_9$	120.1	119.9	$H_8-C_7-C_9$	120.0	119.8
$C_7-C_8-H_9$	120.2	119.8	$C_7-C_9-H_{10}$	119.4	119.7	$C_7-C_9-H_{10}$	120.4	120.0
$C_7-C_8-C_{10}$	120.3	120.2	$C_7-C_9-C_{11}$	121.2	120.5	$C_7-C_9-C_{11}$	120.0	119.9
$H_9-C_8-C_{10}$	119.3	119.8	$H_{10}-C_9-C_{11}$	119.2	119.7	$H_{10}-C_9-C_{11}$	119.5	120.0
$C_8-C_{10}-H_{11}$	120.1	120.3	$C_9-C_{11}-H_{12}$	121.1	121.0	$C_9-C_{11}-H_{12}$	120.9	120.4
$C_8-C_{10}-C_{12}$	118.8	119.3	$C_9-C_{11}-C_{13}$	117.5	117.8	$C_9-C_{11}-C_{13}$	118.8	119.1
$H_{11}-C_{10}-C_{12}$	120.9	120.3	$H_{12}-C_{11}-C_{13}$	121.2	121.0	$H_{12}-C_{11}-C_{13}$	120.1	120.4
$C_{10}-C_{12}-C_{13}$	121.3	120.5	$O_4-H_{12}-C_{11}$	114.2		$C_{11}-C_{13}-C_{14}$	121.4	121.3
$C_{10}-C_{12}-N_{14}$	118.7	112.5	$C_{11}-C_{13}-C_{14}$	122.7	123.6	$C_{11}-C_{13}-N_{15}$	120.6	121.1
$C_{13}-C_{12}-N_{14}$	119.8	120.2	$C_{11}-C_{13}-N_{18}$	118.4	118.8	$C_{14}-C_{13}-N_{15}$	117.8	117.3
$C_6-C_{13}-C_{12}$	119.6	119.7	$C_{14}-C_{13}-N_{18}$	118.8	117.4	$C_6-C_{14}-C_{13}$	119.3	118.9
$C_6-C_{13}-H_{19}$	119.5	120.0	$C_6-C_{14}-C_{13}$	118.6	117.3	$C_6-C_{14}-O_{20}$	124.3	125.4
$C_{12}-C_{13}-H_{19}$	120.7	120.1	$C_6-C_{14}-H_{15}$	119.1	121.3	$C_{13}-C_{14}-O_{20}$	116.3	115.6
$C_{12}-N_{14}-H_{15}$	113.1	109.4	$C_{13}-C_{14}-H_{15}$	122.2	121.3	$C_{13}-N_{15}-H_{16}$	113.0	109.4
$C_{12}-N_{14}-H_{16}$	112.1	109.4	$C_6-O_{16}-H_{17}$	110.2	107.4	$C_{13}-N_{15}-H_{17}$	110.6	109.4
$C_{12}-N_{14}-H_{17}$	113.1	109.5	$C_{13}-N_{18}-H_{19}$	113.0		$C_{13}-N_{15}-H_{18}$	113.0	109.4
$H_{15}-N_{14}-H_{16}$	109.4	109.5	$C_{13}-N_{18}-H_{20}$	112.4		$H_{16}-N_{15}-H_{17}$	110.2	109.4
$H_{15}-N_{14}-H_{17}$	98.74	109.4	$C_{13}-N_{18}-H_{21}$	113.0		$H_{16}-N_{15}-H_{18}$	98.94	109.5
$H_{16}-N_{14}-H_{17}$	109.4	109.4	$H_{19}-N_{18}-H_{20}$	109.5		$H_{17}-N_{15}-H_{18}$	110.3	109.5
$O_5-H_{15}-N_{14}$	144.7		$H_{19}-N_{18}-H_{21}$	98.28		$O_5-H_{16}-N_{15}$	143.9	
$O_4-H_{17}-N_{14}$	143.8		$H_{20}-N_{18}-H_{21}$	109.5		$O_4-H_{18}-N_{15}$	144.2	
$C_7-O_{20}-H_{21}$	110.4	111.4	$O_5-H_{19}-N_{18}$	144.7		$C_{14}-O_{20}-H_{21}$	111.0	

Dihedral angles	4-Hydroxyaniline-$HClO_4$		Dihedral angles	3-Hydroxyaniline-$HClO_4$		Dihedral angles	2-Hydroxyaniline-$HClO_4$	
	B3LYP	X-ray		B3LYP	X-ray		B3LYP	X-ray
$O_2-Cl_1-O_4-H_{17}$	86.27		$O_2-Cl_1-O_4-H_{12}$	42.51		$O_2-Cl_1-O_4-H_{18}$	86.53	
$O_3-Cl_1-O_4-H_{17}$	−149.7		$O_3-Cl_1-O_4-H_{12}$	166.5		$O_3-Cl_1-O_4-H_{18}$	−149.5	
$O_5-ClT_1-O_4-H_{17}$	−30.32		$O_5-Cl_1-O_4-H_{12}$	−74.2		$O_5-Cl_1-O_4-H_{18}$	−30.16	
$O_2-Cl_1-O_5-H_{15}$	−86.24		$O_2-Cl_1-O_5-H_{19}$	−88.0		$O_2-Cl_1-O_5-H_{16}$	−86.48	
$O_3-Cl_1-O_5-H_{15}$	149.83		$O_3-Cl_1-O_5-H_{19}$	147.9		$O_3-Cl_1-O_5-H_{16}$	149.5	
$O_4-Cl_1-O_5-H_{15}$	30.39		$O_4-Cl_1-O_5-H_{19}$	28.75		$O_4-Cl_1-O_5H-H_{16}$	30.19	
$Cl_1-O_4-H_{17}-N_{14}$	13.50		$Cl_1-O_4-H_{12}-C_{11}$	139.5		$Cl_1-O_4-H_{18}-N_{15}$	12.74	
$Cl_1-O_5-H_{15}-N_{14}$	−13.82		$Cl_1-O_5-H_{19}-N_{18}$	−14.5		$Cl_1-O_5-H_{16}-N_{15}$	−12.90	

Table 2 (*Continued*)

Dihedral angles	4-Hydroxyaniline-$HClO_4$		Dihedral angles	3-Hydroxyaniline-$HClO_4$		Dihedral angles	2-Hydroxyaniline-$HClO_4$	
	B3LYP	X-ray		B3LYP	X-ray		B3LYP	X-ray
$C_{13}-C_6-C_7-C_8$	0.001	0.55	$C_{14}-C_6-C_7-H_8$	−179.9		$C_{14}-C_6-C_7-H_8$	180.0	179.2
$C_{13}-C_6-C_7-O_{20}$	−180.0	178.8	$C_{14}-C_6-C_7-C_9$	0.002		$C_{14}-C_6-C_7-C_9$	0.001	0.72
$H_{18}-C_6-C_7-C_8$	−179.9	179.4	$O_{16}-C_6-C_7-H_8$	0.002		$H_{19}-C_6-C_7-C_8$	0.001	0.74
$H_{18}-C_6-C_7-O_{20}$	−0.006	1.13	$O_{16}-C_6-C_7-C_9$	−179.9	−178.6	$H_{19}-C_6-C_7-C_9$	−179.9	−179.2
$C_7-C_6-C_{13}-C_{12}$	−0.002	−0.08	$C_7-C_6-C_{14}-C_{13}$	−0.001	−1.29	$C_7-C_6-C_{14}-C_{13}$	0.007	0.60
$C_7-C_6-C_{13}-H_{19}$	179.9	179.9	$C_7-C_6-C_{14}-H_{15}$	179.9	178.7	$C_7-C_6-C_{14}-O_{20}$	−179.9	−179.8
$H_{18}-C_6-C_{13}-C_{12}$	179.9	179.9	$O_{16}-C_6-C_{14}-C_{13}$	−179.9	179.2	$H_{19}-C_6-C_{14}-C_{13}$	−180.0	−179.3
$H_{18}-C_6-C_{13}-H_{19}$	−0.005	−0.04	$O_{16}-C_6-C_{14}-H_{15}$	0.0007	−0.75	$H_{19}-C_6-C_{14}-O_{20}$	0.004	0.19
$C_6-C_7-C_8-H_9$	179.9	179.2	$C_7-C_6-O_{16}-H_{17}$	0.027	21.16	$C_6-C_7-C_9-H_{10}$	−179.9	−179.6
$C_6-C_7-C_8-C_{10}$	0.002	−0.67	$C_{14}-C_6-O_{16}-H_{17}$	−179.9	−159.2	$C_6-C_7-C_9-C_{11}$	−0.001	−0.33
$O_{20}-C_7-C_8-H_9$	0.002	−1.38	$C_6-C_7-C_9-H_{10}$	180.0	179.4	$H_8-C_7-C_9-H_{10}$	0.0008	−0.36
$O_{20}-C_7-C_8-C_{10}$	−179.9	178.7	$C_6-C_7-C_9-C_{11}$	−0.002	−0.51	$H_8-C_7-C_9-C_{11}$	179.9	179.6
$C_6-C_7-O_{20}-H_{21}$	−179.9	152.7	$H_8-C_7-C_9-H_{10}$	−0.0009	−0.59	$C_7-C_9-C_{11}-H_{12}$	−179.9	−179.2
$C_8-C_7-O_{20}-H_{21}$	0.002	−26.6	$H_8-C_7-C_9-C_{11}$	179.9	179.4	$C_7-C_9-C_{11}-C_{13}$	0.002	−0.16
$C_7-C_8-C_{10}-H_{11}$	179.9	−179.6	$C_7-C_9-C_{11}-H_{12}$	179.9	179.6	$H_{10}-C_9-C_{11}-H_{12}$	0.001	−0.12
$C_7-C_8-C_{10}-C_{12}$	−0.005	0.31	$C_7-C_9-C_{11}-C_{13}$	0.0006	−0.36	$H_{10}-C_9-C_{11}-C_{13}$	179.9	179.8
$H_9-C_8-C_{10}-H_{11}$	−0.001	0.45	$H_{10}-C_9-C_{11}-H_{12}$	−0.007	−0.39	$C_9-C_{11}-C_{13}-C_{14}$	−0.001	0.27
$H_9-C_8-C_{10}-C_{12}$	−179.9	−179.5	$H_{10}-C_9-C_{11}-C_{13}$	179.9	179.6	$C_9-C_{11}-C_{13}-N_{15}$	−179.9	177.4
$C_8-C_{10}-C_{12}-C_{13}$	0.004	0.16	$C_9-C_{11}-H_{12}-O_4$	155.2		$H_{12}-C_{11}-C_{13}-C_{14}$	179.9	−179.7
$C_8-C_{10}-C_{12}-N_{14}$	−179.9	179.3	$C_{13}-C_{11}-H_{12}-O_4$	−24.7		$H_{12}-C_{11}-C_{13}-N_{15}$	−0.001	2.49
$H_{11}-C_{10}-C_{12}-C_{13}$	−179.9	−179.8	$C_9-C_{11}-C_{13}-C_{14}$	0.0007	0.42	$C_{11}-C_{13}-C_{14}-C_6$	0.0001	0.10
$H_{11}-C_{10}-C_{12}-N_{14}$	0.017	0.63	$C_9-C_{11}-C_{13}-N_{18}$	179.9	177.9	$C_{11}-C_{13}-C_{14}-O_{20}$	179.9	179.3
$C_{10}-C_{12}-C_{13}-C_6$	−0.0007	−0.27	$H_{12}-C_{11}-C_{13}-C_{14}$	−179.9	−179.5	$N_{15}-C_{13}-C_{14}-C_6$	179.9	177.0
$C_{10}-C_{12}-C_{13}-H_{19}$	−179.9	179.6	$H_{12}-C_{11}-C_{13}-N_{18}$	−0.001	2.11	$N_{15}-C_{13}-C_{14}-O_{20}$	−0.002	−2.76
$N_{14}-C_{12}-C_{13}-C_6$	179.9	179.2	$C_{11}-C_{13}-C_{14}-C_6$	−0.0003	0.48	$C_{11}-C_{13}-N_{15}-H_{16}$	−55.7	−100.1
$N_{14}-C_{12}-C_{13}-H_{19}$	−0.005	−0.83	$C_{11}-C_{13}-C_{14}-H_{15}$	−180.0	−179.6	$C_{11}-C_{13}-N_{15}-H_{17}$	179.9	19.86
$C_{10}-C_{12}-N_{14}-H_{15}$	−55.34	−38.8	$N_{18}-C_{13}-C_{14}-C_6$	−179.9	−178.7	$C_{11}-C_{13}-N_{15}-H_{18}$	55.62	139.9
$C_{10}-C_{12}-N_{14}-H_{16}$	−179.7	−158.8	$N_{18}-C_{13}-C_{14}-H_{15}$	0.006	−1.26	$C_{14}-C_{13}-N_{15}-H_{16}$	124.2	
$C_{10}-C_{12}-N_{14}-H_{17}$	55.92	81.1	$C_{11}-C_{13}-N_{18}-H_{19}$	−55.32	30.44	$C_{14}-C_{13}-N_{15}-H_{17}$	−0.04	
$C_{13}-C_{12}-N_{14}-H_{15}$	124.6	141.7	$C_{11}-C_{13}-N_{18}-H_{20}$	179.9	150.4	$C_{14}-C_{13}-N_{15}-H_{18}$	−124.3	
$C_{13}-C_{12}-N_{14}-H_{16}$	0.296	21.6	$C_{11}-C_{13}-N_{18}-H_{21}$	55.26	151.1	$C_6-C_{14}-O_{20}-H_{21}$	−0.043	
$C_{13}-C_{12}-N_{14}-H_{17}$	−124.0	−98.3	$C_{14}-C_{13}-N_{18}-H_{19}$	124.6	88.2	$C_{13}-C_{14}-O_{20}-H_{21}$	179.9	
$C_{12}-N_{14}-H_{15}-O_5$	113.1		$C_{14}-C_{13}-N_{18}-H_{20}$	−0.04	31.2	$C_{13}-N_{15}-H_{16}-O_5$	111.9	
$H_{16}-N_{14}-H_{15}-O_5$	−121.0		$C_{14}-C_{13}-N_{18}-H_{21}$	−124.7	89.5	$H_{17}-N_{15}-H_{16}-O_5$	−123.5	
$H_{17}-N_{14}-H_{15}-O_5$	−6.794		$C_{13}-N_{18}-H_{19}-O_5$	115.2		$H_{18}-N_{15}-H_{16}-O_5$	−7.89	
$C_{12}-N_{14}-H_{17}-O_4$	−112.9		$H_{20}-N_{18}-H_{19}-O_5$	−118.4		$C_{13}-N_{15}-H_{18}-O_4$	−111.8	
$H_{15}-N_{14}-H_{17}-O_4$	6.929		$H_{21}-N_{18}-H_{19}-O_5$	−4.22		$H_{16}-N_{15}-H_{18}-O_4$	8.012	
$H_{16}-N_{14}-H_{17}-O_4$	121.1					$H_{17}-N_{15}-H_{18}-O_4$	123.6	

Table 3
Vibrational frequencies of 2-hydroxyanilinium perchlorate.

	Scaled freq.[a]	I_{IR} [b]	Exp. IR	TED[c] (%)	Assignment
ν_1	36	0.20		$\delta_{OHN}(59)+\Gamma_{HNCC}(41)$	δ(hydrogen bridge) + tor(ϕ-NH_3)
ν_2	42	0.00		$\Gamma_{NHOC}(66)+\Gamma_{HNCC}(34)$	tor(ϕ-NH_3)
ν_3	52	0.08		$\Gamma_{HOCO}(68)+\delta_{COH}(15)+\Gamma_{NHOC}(12)$	tor(H—O—C—O)
ν_4	64	0.43	94m	$\Gamma_{OHNC}(50)+\Gamma_{OHNH}(32)+\Gamma_{OCOH}(18)$	tor(ϕ)
ν_5	121	0.01		$\delta_{OHN}(23)+\Gamma_{HNCC}(22)+\Gamma_{NHOC}(18)+\nu_{OH}(12)$	tor(ϕ-NH_3)
ν_6	155	1.68	133m	$\nu_{OH}(56)+\delta_{NCC}(21)+\delta_{HOC}(13)$	$\delta(\phi)$
ν_7	183	2.18	218m	$\Gamma_{NHOC}(33)+\Gamma_{OCCC}(16)+\Gamma_{CCCC}(15)+\Gamma_{OCCN}(11)$	tor(ϕ-NH_3) + tor(ϕ-OH) + tor(ϕ)
ν_8	242	6.15	290m	$\Gamma_{HOCC}(68)+\Gamma_{OCCC}(12)$	tor(ϕ-OH)
ν_9	278	0.50		$\Gamma_{HOCC}(21)+\Gamma_{NCCC}(19)+\Gamma_{OCCC}(17)+\Gamma_{NHOC}(15)$	tor(ϕ-OH) + tor(ϕ-NH_3)
ν_{10}	345	6.76	322m	$\delta_{OCC}(25)+\nu_{OH}(17)+\delta_{CCC}(15)+\delta_{HOC}(12)$	δ(ϕ-OH) + δ(ϕ-NH_3)
ν_{11}	355	1.16		$\delta_{OClO}(45)+\delta_{ClOH}(32)$	$\nu_2 ClO_4^-$
ν_{12}	399	0.33		$\delta_{OClO}(50)+\delta_{ClOH}(36)$	$\nu_2 ClO_4^-$
ν_{13}	415	2.85	417w	$\delta_{OClO}(75)+\nu_{OH}(15)$	$\nu_2 ClO_4^-$
ν_{14}	428	0.07	434m448w	$\delta_{OCC}(37)+\delta_{NCC}(21)$	δ(ϕ-OH) + δ(ϕ-NH_3)
ν_{15}	438	1.39	440m	$\Gamma_{CCCC}(36)+\Gamma_{CCCH}(21)$	$\gamma(\phi)$
			466w		
			457vw		
ν_{16}	527	0.77	539w	$\delta_{OClO}(55)+\Gamma_{HOClO}(22)$	$\nu_4 ClO_4^-$
ν_{17}	532	0.19	544m	$\Gamma_{CCCC}(25)+\delta_{OClO}(22)$	$\nu_4 ClO_4^- + \gamma(\phi)$
			580vw		
ν_{18}	535	0.70	616sh	$\delta_{OClO}(49)$	$\nu_4 ClO_4^-$
			606wsh		
ν_{19}	537	1.95	627vs	$\delta_{CCC}(24)+\delta_{OCC}(16)+\delta_{CCN}(14)+\delta_{OClO}(11)$	$\nu_4 ClO_4^-$ + $\delta(\phi)$ + δ(ϕ-OH) + tor NH_3
ν_{20}	552	6.97	634ssh	$\delta_{OClO}(70)+\Gamma_{HOClO}(17)$	$\nu_4 ClO_4^-$
ν_{21}	567	0.98		$\delta_{CCC}(41)+\delta_{CCH}(12)$	$\delta(\phi)$
ν_{22}	690	0.01	714w	$\Gamma_{CCCC}(48)+\Gamma_{CCCH}(23)$	$\gamma(\phi)$
ν_{23}	745	4.62	743s	$\Gamma_{CCCH}(70)+\Gamma_{OCCH}(15)$	ωC—H
ν_{24}	745	0.12		$\nu_{CC}(42)+\nu_{NC}(20)+\nu_{OC}(10)$	νC—C + νC—N + νC—O
ν_{25}	761	6.87	757s	$\nu_{OCl}(93)$	$\nu_1 ClO_4^-$
ν_{26}	825	15.24	752vs	$\nu_{OCl}(56)$	$\nu_1 ClO_4^-$

Table 3 (*Continued*)

	Scaled freq.[a]	I_{IR} [b]	Exp. IR	TED[c] (%)	Assignment
ν_{27}	827	1.23	834vwb	$\delta_{CCC}(39)+\nu_{OC}(18)+\delta_{CCH}(12)+\nu_{NC}(11)$	$\delta(\phi)+\nu$C—O + νC—N
ν_{28}	840	5.72	858w	$\delta_{CCCH}(35)+\nu_{OC}(17)+\mathit{\Gamma}_{HCCH}(17)$	ωC—H
			849m		
			842w		
			884w		
ν_{29}	939	0.37	936w	$\mathit{\Gamma}_{HCCH}(55)+\mathit{\Gamma}_{CCCH}(33)$	τC—H
			932vw		
ν_{30}	947	25.73	941w	$\nu_{OCl}(90)$	$\nu_3ClO_4^-$
ν_{31}	979	0.10	980w	$\mathit{\Gamma}_{HCCH}(59)+\mathit{\Gamma}_{CCCH}(19)$	$\tau(\phi)$
			1016msh		
			1006m		
ν_{32}	1021	4.29	1041ssh	$\nu_{CC}(55)+\delta_{CCH}(15)$	νC—C + ρC—H
			1030ssh		
			1072vs		
ν_{33}	1043	15.33	1089vs	$\nu_{OCl}(62)+\nu_{CC}(11)$	$\nu_3ClO_4^-+\nu$C—C
ν_{34}	1048	13.50	1106vs	$\upsilon_{OCl}(23)+\nu_{CC}(13)+\delta_{CNH}(12)$	$\nu_3ClO_4^-+\nu$C—C + δ_aNH_3, γN—H···O
ν_{35}	1050	0.01		$\delta_{CNH}(44)+\mathit{\Gamma}_{CCNH}(24)+\mathit{\Gamma}_{CNHO}(14)$	δ_aNH_3, δN—H···O
ν_{36}	1100	8.20	1123vssh	$\delta_{COH}(30)+\nu_{CC}(21)$	δO—H + νC—C, δO—H···O, 2.8245 Å
ν_{37}	1145	0.54	1157vssh	$\delta_{CCH}(63)+\nu_{CC}(22)$	sciss C—H + νC—C
ν_{38}	1159	1.28	1172s	$\delta_{CCH}(64)+\nu_{CC}(19)$	sciss C—H + νC—C
			1195w		
ν_{39}	1185	2.51	1225s	$\nu_{NC}(32)+\delta_{COH}(26)+\nu_{CC}(22)$	δO—H + νC—N + νC—C, δO—H···O, 2.8245 Å
			1230ssh		
ν_{40}	1252	7.52	1264w	$\nu_{OC}(43)+\nu_{CC}(22)+\delta_{CCH}(19)$	νC—O + νC—C + ρC—H
			1280vs		
			1291ssh		
ν_{41}	1310	2.99	1315m	$\nu_{CC}(75)+\delta_{CCH}(10)$	νC—C + sciss C—H
ν_{42}	1321	1.88	1342s	$\delta_{CCH}(54)+\delta_{COH}(20)$	ρC—H + δO—H, δO—H···O, 2.8245 Å
ν_{43}	1451	2.40	1482vs	$\delta_{CCH}(45)+\nu_{CC}(32)$	ρC—H + νC—C
ν_{44}	1491	8.54	1468vs	$\delta_{CCH}(47)+\nu_{CC}(26)$	ρC—H + νC—C
			1498vs		
ν_{45}	1535	16.21	1522m	$\mathit{\Gamma}_{HNHO}(37)+\delta_{HNH}(35)+\delta_{CNH}(29)$	δ_sNH_3, δN—H···O
			1515m		
			1510s		
ν_{46}	1572	1.92	1569w	$\delta_{HNH}(51)+\delta_{CNH}(17)+\mathit{\Gamma}_{CCNH}(15)$	δ_aNH_3, δN—H···O
			1574w		
ν_{47}	1591	14.41	1594m	$\nu_{CC}(38)+\delta_{HNH}(20)+\mathit{\Gamma}_{HNCC}(13)$	νC—C + $\delta_aNH_3+\delta(\phi)$, δN—H···O
ν_{48}	1594	2.09	1606m	$\nu_{CC}(51)+\delta_{HNH}(11)$	νC—C + δ_aNH_3, δN—H···O
ν_{49}	1620	15.79	1635s	$\nu_{CC}(37)+\delta_{HNH}(22)$	νC—C + δ_aNH_3, δN—H···O
			1630msh		
ν_{50}	2839	9.58	3114s	$\nu_{NH}(96)$	ν_sNH_3, νN—H···O
ν_{51}	2927	100	3181s	$\nu_{NH}(98)$	ν_sNH_3, νN—H···O
ν_{52}	3024	0.37	3016s	$\nu_{CH}(98)$	νC—H aromatic
			2998s		
ν_{53}	3028	3.99	3030s	$\nu_{CH}(97)$	νC—H aromatic
ν_{54}	3045	0.07	3049s	$\nu_{CH}(98)$	νC—H aromatic
ν_{55}	3061	0.37	3067s	$\nu_{CH}(97$	νC—H aromatic
ν_{56}	3331	8.00	3229ssh	$\nu_{NH}(100)$	ν_aNH_3, νN—H···O
ν_{57}	3669	8.67	3441m	$\nu_{OH}(100)$	νO—H···O, 2.8245 Å

ν, stretching; a, antisymmetric; s, symmetric; δ, in-plane bending; γ, out-of-plane bending, ϕ, benzene ring; lib, librational; tor, torsional; τ, twisting; ω, wagging; ρ, rocking; sciss, scissoring.

[a] Obtained from the wave numbers calculated at B3LYP/6-311++G(d,p) using scaling factors 0.967 (for wave numbers under 1800 cm^{-1}) and 0.955 (for those over 1800 cm^{-1}).

[b] Relative absorption intensities normalized with highest peak absorption equal to 100.

[c] Total energy distribution calculated B3LYP/6-311++G(d,p) level of theory. Only contributions ≥10% are listed.

2.3. *Differential scanning calorimetry*

The DSC measurements were performed in the temperature range 80–293 K on Perkin Elmer DSC 7 instrument.

3. Computational details

Gaussian 09 quantum chemical software was used in all calculations [14]. The optimized structural parameters and vibrational wavenumbers for the 2, 3 and 4-hydroxyanilinium perchlorate compounds were calculated by using B3LYP functional with 6-311++G(d,p) as basis sets. The vibrational modes were assigned on the basis of total energy distribution (TED) analysis using scaled quantum mechanics (SQM) program [15]. The calculated vibrational wavenumbers were scaled with 0.967 (for wavenumbers under 1800 cm^{-1}) and 0.955 (for those over 1800 cm^{-1}) for B3LYP/6-311++G(d,p) in order to figure out how the calculated data were in agreement with those of the experimental ones [16,17].

4. Results and discussion

4.1. *Structural remarks*

The crystal structures of 2-, 3- and 4-hydroxyanilinium perchlorate (2HAP-ClO_4, 3HAP-ClO_4 and 4HAP-ClO_4) have been recently published by Janczak and Perpetuo [18]. It seems to be worthwhile mentioning here that the hydrogen bonding network is sometimes important in the enhancement of the hyperpolarizability of the hydroxyanilinium cations and can influence on non-linear optical (NLO) properties of crystals [18]. For better characterization of hydrogen bonds in this work we additionally focused on the graph-set analysis of the hydrogen bond patterns [21].

The studied compounds crystallize in centrosymmetric (2HAP-ClO_4 $C2/c$) and non-centrosymmetric (3HAP-ClO_4 $P2_1$, 4HAP-ClO_4 $P2_12_12_1$) space groups. In 2HAP-ClO_4, a chain pattern of hydrogen bonds, $C^2{}_2(6)$, is constructed parallel to the c axis (Table 1). The compounds create the pattern are transformed by the c-glide plane which is perpendicular to the main axis b in the $C2/c$ space group. The second binary pattern is a helical chain, $C^2{}_2(9)$, parallel to the b axis. The left-handed helical chain of hydrogen bonds is wound round the screw axis 2_1 located at ¼, b, ¼ position. The second left-handed helix is generated at ¾, b, ¼ position by the two-fold axis. Due to the centrosymmetry, the two left-handed helixes transform to two right-handed helixes. As a result, four helical chains $C^2{}_2(9)$ around the 2_1 screw axes exist in the unit cell.

In the case of 3HAP-ClO_4, the only one non-trivial symmetry element in $P2_1$ space group exists, namely 2_1 screw axis parallel to the crystallographic b axis. The 3-hydroxyanilinium cations are arranged around this screw axis resulting in the left-handed helically structured chain pattern, which is designated by the unitary graph-set C(6). The perchlorate anions beside the organic cations are involved in creation of the chains $C^2{}_2(6)$, $C^2{}_2(10)$ and the other $C^2{}_2(10)$. These three chains are formed by the organic and inorganic ions transformed by translation vectors along b, c and $[0\,1\,\bar{1}]$ directions, respectively.

The 4HAP-ClO_4 crystallizes in $P2_12_12_1$ space group and therefore the patterns of hydrogen bonds existing in the crystal structure are wound round these screw axes. Six binary graph-sets designate the patterns constructed by the 4-hydroxyanilinium cations and perchlorate anions, *e.g.* three $C^2{}_2(6)$, one $C^1{}_2(9)$ and two $C^2{}_2(11)$. The only one pattern is formed by the translation vector along the crystallographic a axis.

In the studied SHG active compounds, 3HAP-ClO_4 and 4HAP-ClO_4, helically structured patterns of hydrogen bonds occur. Interestingly, in the 2HAP-ClO_4 complex one hydrogen bonding pattern is constructed in a helical manner. Unfortunately, the existence of the inversion centre in the structure excludes the second harmonic generation in such a case. It is worth noticing that in the studied non-centrosymmetric structures, the twist of the particular helix is changed in the enantiomorphic crystal, *i.e.* the left-handed helix changes to the right-handed one and *vice versa*. NLO properties remain unchanged in such situation.

4.2. Molecular geometries

The optimized structures of 2HAP-ClO_4, 3HAP-ClO_4 and 4HAP-ClO_4 are shown in Fig. 1. The optimized geometric parameters of these compounds are collected in Table 2. These optimized geometric parameters of these compounds are compared with X-ray data [18].

4.3. Vibrational analysis

The spectroscopic properties of 2HAP-ClO_4, 3HAP-ClO_4 and 4HAP-ClO_4 have not yet been studied in detail to the best of our knowledge. These compounds consist of 21 atoms, which have 57 vibrational degrees of freedom. The 57 normal modes of these compounds have been assigned according to the detailed vibrations of the individual atoms. These compounds belong to C_1 symmetry group. Scale factors were used to fit the calculated wavenumbers with observed. Fig. 2 presents the FT-IR spectra of these compounds, respectively. The experimental Far infrared and FT-IR wavenumbers are tabulated in Tables 3–5, together with the calculated wavenumbers. As it can be seen in tables IR absorption intensities of these compounds are in consistency with the TED results.

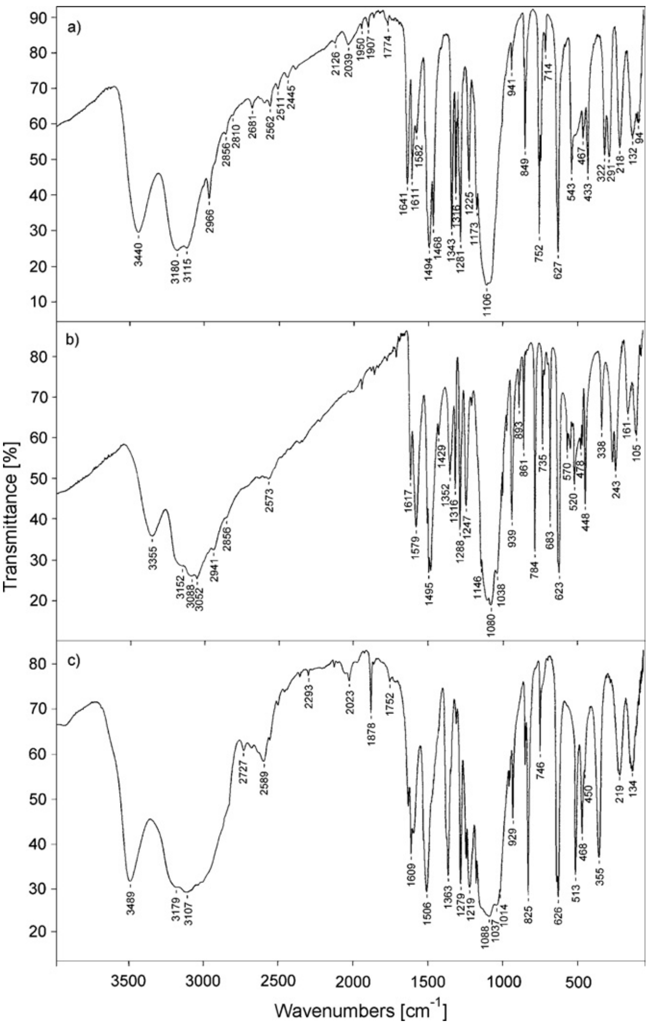

Fig. 2. FT-IR spectra of 2-hydroxyanilinium perchlorate (a), 3-hydroxyanilinium perchlorate (b) and 4-hydroxyanilinium perchlorate (c).

Nine normal modes of perchlorate anion of T_d symmetry are manifested by four bands (ν_1, ν_2, ν_3 and ν_4) in vibrational spectra. The ν_1 and ν_2 modes Raman active, whereas ν_3 and ν_4 vibrations are active in both infrared and Raman spectra. The frequencies corresponding to above vibrations are as follows: $\nu_1 = 928\,cm^{-1}$, $\nu_2 = 459\,cm^{-1}$, $\nu_3 = 119\,cm^{-1}$ and $\nu_4 = 625\,cm^{-1}$. X-ray data show that the perchlorate anions occupy a position of C_1 symmetry. Since of this, the degeneracy of doubly degenerate bending (ν_2) and triply degenerate stretching and bending (ν_3 and ν_4) modes should be observed. ν_1 vibration one can expect in infrared and Raman spectra. Therefore, nine bands due to internal vibrations of perchlorate anion should be observed in the vibrational spectra. $1119\,cm^{-1}$ and $928\,cm^{-1}$ peaks were assigned to the antisymmetric and symmetric stretching vibrations, respectively. $625\,cm^{-1}$ and $459\,cm^{-1}$ peaks were assigned to the in-plane and out-of-plane deformation vibrations, respectively [19,20].

It is reduced to C_1 symmetry from T_d symmetry. Under this circumstance, all of the vibrations are active in both FT-IR and FT-Raman spectra. The very board band at approximately $1100\,cm^{-1}$ is characteristic for all spectra. These vibrations were assigned to the antisymmetric stretching mode ($\nu_3 = 1119\,cm^{-1}$). These absorption is divided into three different submaxima. The antisymmetric stretching modes of perchloric acid are observed at $1106\,cm^{-1}$, $1089\,cm^{-1}$ and $947\,cm^{-1}$ for 2HAP-ClO_4 in the FT-IR spectra. These modes are observed at $1147\,cm^{-1}$ ($1172\,cm^{-1}$), $1106\,cm^{-1}$ and $1080\,cm^{-1}$ for 3HAP-ClO_4 and $1087\,cm^{-1}$, $1013\,cm^{-1}$ and $1037\,cm^{-1}$ for 4HAP-ClO_4. In-plane deformation vibrations of

Table 4
Vibrational frequencies of 3-hydroxyanilinium perchlorate.

	Scaled freq.[a]	I_{IR} [b]	Exp. IR	TED[c] (%)	Assignment
ν_1	26	0.28		$\Gamma_{\mathrm{CCNH}}(60)+\delta_{\mathrm{NHO}}(37)$	δ(hydrogen bridge) + lib (3-aminophenol)
ν_2	41	0.02		$\Gamma_{\mathrm{ClOHN}}(45)+\delta_{\mathrm{NHO}}(26)+\Gamma_{\mathrm{CCNH}}(24)$	lib $\mathrm{ClO_4^-}$ + tor(ϕ-$\mathrm{NH_3}$)
ν_3	44	0.15		$\Gamma_{\mathrm{OClOH}}(53)+\delta_{\mathrm{ClOH}}(13)+\Gamma_{\mathrm{HNHO}}(12)$	lib $\mathrm{ClO_4^-}$ + tor(ϕ-$\mathrm{NH_3}$)
ν_4	61	0.50		$\Gamma_{\mathrm{OClOH}}(57)+\Gamma_{\mathrm{OHNH}}(41)$	tor ϕ
ν_5	116	0.06		$\delta_{\mathrm{NHO}}(27)+\Gamma_{\mathrm{CCCH}}(15)+\nu_{\mathrm{OH}}(13)+\Gamma_{\mathrm{NCCH}}(10)$	tor(ϕ-$\mathrm{NH_3}$)
ν_6	163	1.71		$\nu_{\mathrm{OH}}(55)+\delta_{\mathrm{CCN}}(20)+\delta_{\mathrm{HOCl}}(15)$	δ(ϕ-OH) + δ(ϕ-$\mathrm{NH_3}$)
ν_7	222	0.20		$\Gamma_{\mathrm{OCCC}}(48)+\Gamma_{\mathrm{CCCC}}(18)$	$\gamma(\phi)$
ν_8	232	0.78		$\Gamma_{\mathrm{ClOHN}}(39)+\Gamma_{\mathrm{CCCN}}(30)+\Gamma_{\mathrm{CCCC}}(17)$	tor(ϕ-$\mathrm{NH_3}$) + $\gamma(\phi)$
ν_9	325	7.93		$\Gamma_{\mathrm{CCOH}}(99)$	γO—H
ν_{10}	340	5.27		$\delta_{\mathrm{OCC}}(30)+\delta_{\mathrm{CCN}}(22)+\nu_{\mathrm{OH}}(14)$	δ(ϕ-OH) + δ(ϕ-$\mathrm{NH_3}$)
ν_{11}	355	0.60		$\delta_{\mathrm{OClO}}(58)+\delta_{\mathrm{ClOH}}(30)$	$\nu_2\mathrm{ClO_4^-}$ + tor $\mathrm{NH_3}$
ν_{12}	400	0.24		$\delta_{\mathrm{OClO}}(46)+\delta_{\mathrm{HOCl}}(42)$	$\nu_2\mathrm{ClO_4^-}$ + tor $\mathrm{NH_3}$
ν_{13}	413	1.69	409w	$\delta_{\mathrm{OClO}}(78)+\delta_{\mathrm{OCC}}(10)+\nu_{\mathrm{OH}}(10)$	$\nu_2\mathrm{ClO_4^-}$ + δ(ϕ-OH)
ν_{14}	439	0.37	425w429w	$\Gamma_{\mathrm{CCCH}}(71)$	$\gamma(\phi)$
ν_{15}	456	0.70	448s 467w 478w	$\delta_{\mathrm{OCC}}(38)+\delta_{\mathrm{CCN}}(26)$	δ(ϕ-$\mathrm{NH_3}$) + δ(ϕ-OH)
ν_{16}	508	0.08	520m	$\delta_{\mathrm{CCC}}(47)+\delta_{\mathrm{CCH}}(10)$	$\delta(\phi)$ + δC—H
ν_{17}	527	1.14	537w	$\delta_{\mathrm{OClO}}(42)+\delta_{\mathrm{CCC}}(11)$	$\nu_4\mathrm{ClO_4^-}$ + $\delta(\phi)$
ν_{18}	534	1.03	549m 555msh	$\delta_{\mathrm{OClO}}(22)+\delta_{\mathrm{CCC}}(21)$	$\nu_4\mathrm{ClO_4^-}$ + $\delta(\phi)$
ν_{19}	534	0.68	569m	$\delta_{\mathrm{OClO}}(72)+\nu_{\mathrm{OCl}}(15)$	$\nu_4\mathrm{ClO_4^-}$
ν_{20}	555	8.63	623vs 629vs	$\delta_{\mathrm{OClO}}(60)+\Gamma_{\mathrm{OClOH}}(35)$	$\nu_4\mathrm{ClO_4^-}$
ν_{21}	559	0.20	683s 699vw	$\Gamma_{\mathrm{CCCH}}(20)+\Gamma_{\mathrm{CCCC}}(17)+\Gamma_{\mathrm{NCCC}}(10)$	$\gamma(\phi)$
ν_{22}	662	1.46	735m 784vs 832vw	$\Gamma_{\mathrm{CCCC}}(52)+\Gamma_{\mathrm{CCCH}}(36)$	ωC—H
ν_{23}	720	0.70	846vw	$\delta_{\mathrm{CCC}}(28)+\nu_{\mathrm{CC}}(21)+\nu_{\mathrm{NC}}(14)$	$\delta(\phi)$ + νC—C + νC—N
ν_{24}	758	7.00	861m	$\nu_{\mathrm{CCl}}(90)$	$\nu_1\mathrm{ClO_4^-}$
ν_{25}	764	1.33	888w 892w	$\Gamma_{\mathrm{CCCH}}(60)+\Gamma_{\mathrm{OCCH}}(17)+\Gamma_{\mathrm{NCCH}}(10)$	ωC—H
ν_{26}	811	9.04	939s	$\nu_{\mathrm{OCl}}(49)+\Gamma_{\mathrm{CCCH}}(10)$	$\nu_1\mathrm{ClO_4^-}$ + γC—H
ν_{27}	831	11.46	943s	$\Gamma_{\mathrm{OCCH}}(22)+\nu_{\mathrm{OCl}}(21)+\Gamma_{\mathrm{CCCH}}(19)+\Gamma_{\mathrm{NCCH}}(18)$	γC—H + $\nu_1\mathrm{ClO_4^-}$
ν_{28}	872	1.00	974w 1001s	$\Gamma_{\mathrm{CCCH}}(37)+\Gamma_{\mathrm{HCCH}}(23)+\Gamma_{\mathrm{NCCH}}(13)$	τC—H
ν_{29}	926	2.85	1038vs	$\nu_{\mathrm{CC}}(31)+\nu_{\mathrm{NC}}(19)+\nu_{\mathrm{OC}}(15)$	νC—C + νC—N + νC—O
ν_{30}	950	22.68	1080vs	$\nu_{\mathrm{OCl}}(87)$	$\nu_3\mathrm{ClO_4^-}$
ν_{31}	963	0.04		$\Gamma_{\mathrm{HCCH}}(59)+\Gamma_{\mathrm{CCCH}}(23)$	τC—H
ν_{32}	980	0.48		$\nu_{\mathrm{CC}}(42)+\delta_{\mathrm{CCC}}(35)$	νC—C + $\delta(\phi)$
ν_{33}	1039	0.01		$\delta_{\mathrm{CNH}}(42)+\Gamma_{\mathrm{CCNH}}(28)$	$\delta_a\mathrm{NH_3}$, δN—H···O
ν_{34}	1045	30.29	1106vs	$\nu_{\mathrm{OCl}}(78)$	$\nu_3\mathrm{ClO_4^-}$
ν_{35}	1056	1.62	1147vs 1172m	$\delta_{\mathrm{CNH}}(32)+\nu_{\mathrm{CC}}(21)+\Gamma_{\mathrm{OHNH}}(20)+\nu_{\mathrm{OCl}}(11)$	$\delta_a\mathrm{NH_3}$ + νC—C + $\nu_3\mathrm{ClO_4^-}$, δN—H···O
ν_{36}	1090	0.05	1210w	$\delta_{\mathrm{CCH}}(35)+\nu_{\mathrm{CC}}(32)$	sciss C—H + νC—C
ν_{37}	1130	4.60	1247s	$\delta_{\mathrm{CCH}}(41)+\nu_{\mathrm{NC}}(22)+\nu_{\mathrm{CC}}(13)+\nu_{\mathrm{OC}}(12)$	δC—H + νC—N + νC—C + νC—O
ν_{38}	1152	4.01	1277m	$\delta_{\mathrm{COH}}(38)+\delta_{\mathrm{CCH}}(30)+\nu_{\mathrm{CC}}(23)$	δO—H + sciss C—H + νC—C, δO—H···O, 2.7943 Å
ν_{39}	1167	3.13	1289s	$\delta_{\mathrm{CCH}}(48)+\nu_{\mathrm{CC}}(20)+\delta_{\mathrm{COH}}(19)$	δO—H + sciss C—H + νC—C, δO—H···O, 2.7943 Å
ν_{40}	1264	4.30	1317m	$\nu_{\mathrm{OC}}(40)+\nu_{\mathrm{CC}}(17)+\delta_{\mathrm{CCH}}(10)$	νC—O + νC—C + sciss C—H
ν_{41}	1309	1.58	1343w 1352m	$\delta_{\mathrm{CCH}}(78)$	ρC—H
ν_{42}	1318	1.47	1364m	$\nu_{\mathrm{CC}}(65)+\delta_{\mathrm{COH}}(17)$	νC—C + δO—H, δO—H···O, 2.7943 Å
ν_{43}	1473	2.79	1480vs	$\delta_{\mathrm{CCH}}(35)+\nu_{\mathrm{CC}}(28)$	ρC—H + νC—C
ν_{44}	1475	6.64	1494vs	$\delta_{\mathrm{CCH}}(45)+\nu_{\mathrm{CC}}(33)$	ρC—H + νC—C
ν_{45}	1539	32.30	1503s	$\delta_{\mathrm{HNH}}(39)+\Gamma_{\mathrm{HNHO}}(30)+\delta_{\mathrm{CNH}}(26)$	$\delta_s\mathrm{NH_3}$, δN—H···O
ν_{46}	1567	1.74	1540w	$\delta_{\mathrm{HNH}}(51)+\delta_{\mathrm{CNH}}(19)+\Gamma_{\mathrm{ClOHN}}(15)$	$\delta_a\mathrm{NH_3}$, δN—H···O
ν_{47}	1590	4.62	1560msh	$\nu_{\mathrm{CC}}(61)$	νC—C
ν_{48}	1598	21.17	1580vs	$\delta_{\mathrm{NHN}}(35)+\nu_{\mathrm{CC}}(30)+\Gamma_{\mathrm{HNHO}}(15)+\Gamma_{\mathrm{CCNH}}(14)$	νC—C + $\delta_a\mathrm{NH_3}$, δN—H···O
ν_{49}	1620	3.61	1617m	$\nu_{\mathrm{CC}}(30)+\delta_{\mathrm{HNH}}(27)+\Gamma_{\mathrm{CCNH}}(14)$	νC—C + $\delta_a\mathrm{NH_3}$, δN—H···O
ν_{50}	2796	9.25	3102s	$\nu_{\mathrm{NH}}(98)$	$\nu_s\mathrm{NH_3}$, νN—H···O
ν_{51}	2896	100	3110s	$\nu_{\mathrm{NH}}(99)$	$\nu_s\mathrm{NH_3}$, νN—H···O
ν_{52}	3021	0.78		$\nu_{\mathrm{CH}}(99)$	νC—H aromatic
ν_{53}	3038	2.18	3053s	$\nu_{\mathrm{CH}}(95)$	νC—H aromatic
ν_{54}	3040	0.13		$\nu_{\mathrm{CH}}(96)$	νC—H aromatic
ν_{55}	3054	0.45	3064s	$\nu_{\mathrm{CH}}(99)$	νC—H aromatic
ν_{56}	3361	4.05	3169s	$\nu_{\mathrm{NH}}(99)$	$\nu_a\mathrm{NH_3}$, νN—H···O
ν_{57}	3660	6.63	3357m	$\nu_{\mathrm{OH}}(100)$	νO—H···O, 2.7943 Å

ν, stretching; a, antisymmetric; s, symmetric; δ, in-plane bending; γ, out-of-plane bending, ϕ, benzene ring; lib, librational; tor, torsional; τ, twisting; ω, wagging; ρ, rocking; sciss, scissoring.

[a] Obtained from the wave numbers calculated at B3LYP/6-311++G(d,p) using scaling factors 0.967 (for wave numbers under 1800 cm^{-1}) and 0.955 (for those over 1800 cm^{-1}).

[b] Relative absorption intensities normalized with highest peak absorption equal to 100.

[c] Total energy distribution calculated B3LYP/6-311++G(d,p) level of theory. Only contributions ≥10% are listed.

Table 5
Vibrational frequencies of 4-hydroxyanilinium perchlorate.

	Scaled freq.[a]	I_{IR} [b]	Exp. IR	TED[c] (%)	Assignment
ν_1	37	0.41		$\delta_{\mathrm{NHO}}(58)+\Gamma_{\mathrm{CCNH}}(32)$	lib $\mathrm{ClO_4}^-$ + tor $\mathrm{NH_3}$
ν_2	43	0.03		$\Gamma_{\mathrm{ClOHN}}(52)+\Gamma_{\mathrm{CCNH}}(47)$	lib $\mathrm{ClO_4}^-$ + tor $\mathrm{NH_3}$
ν_3	52	0.32		$\Gamma_{\mathrm{OHNC}}(31)+\Gamma_{\mathrm{OHNH}}(29)+\Gamma_{\mathrm{OClOH}}(26)$	lib $\mathrm{ClO_4}^-$ + lib (4-aminophenol)
ν_4	59	0.47		$\Gamma_{\mathrm{OClOH}}(52)+\Gamma_{\mathrm{OHNH}}(33)$	lib $\mathrm{ClO_4}^-$ + lib (4-aminophenol)
ν_5	94	0.04		$\delta_{\mathrm{NHO}}(38)+\Gamma_{\mathrm{ClOHN}}(35)+\Gamma_{\mathrm{NCCC}}(12)+\nu_{\mathrm{OH}}(10)$	$\nu_2\mathrm{ClO_4}^-$ + tor $\mathrm{NH_3}$
ν_6	163	0.29		$\Gamma_{\mathrm{ClOHN}}(54)+\Gamma_{\mathrm{CCCO}}(20)+\Gamma_{\mathrm{CCCC}}(17)$	tor $\mathrm{NH_3}$
ν_7	177	2.79		$\nu_{\mathrm{OH}}(64)+\delta_{\mathrm{CCN}}(18)$	$\delta(\phi\text{-}\mathrm{NH_3})+\nu$O—H
ν_8	319	0.24		$\Gamma_{\mathrm{ClOHN}}(24)+\delta_{\mathrm{ClOH}}(24)+\Gamma_{\mathrm{CCNH}}(16)+\Gamma_{\mathrm{OCCC}}(13)$	γO—H + tor $\mathrm{NH_3}$
ν_9	332	7.27		$\delta_{\mathrm{ClOH}}(25)$	γO—H
ν_{10}	347	3.73		$\Gamma_{\mathrm{CCOH}}(92)$	$\delta(\phi\text{-}\mathrm{NH_3})+\delta(\phi\text{-OH})$
ν_{11}	355	2.79		$\delta_{\mathrm{OCC}}(32)+\delta_{\mathrm{NCC}}(28)+\nu_{\mathrm{OH}}(10)$	tor $\mathrm{NH_3}$
ν_{12}	396	0.37		$\delta_{\mathrm{OClO}}(47)+\Gamma_{\mathrm{NCCC}}(13)$	$\nu_2\mathrm{ClO_4}^-$ + tor $\mathrm{NH_3}$
ν_{13}	409	0.62	411s	$\delta_{\mathrm{OClO}}(61)+\delta_{\mathrm{ClOH}}(30)$	$\nu_2\mathrm{ClO_4}^-$
ν_{14}	409	0.07	429m	$\delta_{\mathrm{OClO}}(73)+\delta_{\mathrm{OCC}}(16)$	$\gamma(\phi)$
ν_{15}	434	1.38	448s	$\Gamma_{\mathrm{CCCC}}(53)+\Gamma_{\mathrm{CCCH}}(22)$	$\delta(\phi\text{-}\mathrm{NH_3})$
ν_{16}	461	3.59	460m477s	$\delta_{\mathrm{OCC}}(28)+\delta_{\mathrm{NCC}}(26)+\delta_{\mathrm{CCC}}(11)$	$\delta(\phi)$
ν_{17}	499	2.13	507s	$\delta_{\mathrm{CCC}}(37)+\delta_{\mathrm{CCN}}(15)+\nu_{\mathrm{OH}}(10)$	$\gamma(\phi)$
ν_{18}	529	1.93		$\Gamma_{\mathrm{CCCH}}(39)+\Gamma_{\mathrm{CCCC}}(19)+\Gamma_{\mathrm{CCCO}}(10)$	$\nu_4\mathrm{ClO_4}^-$
ν_{19}	535	1.07		$\delta_{\mathrm{OClO}}(63)+\delta_{\mathrm{ClOH}}(22)$	$\nu_4\mathrm{ClO_4}^-$
ν_{20}	553	7.09	625vs	$\delta_{\mathrm{OClO}}(69)+\nu_{\mathrm{OCl}}(15)$	$\nu_4\mathrm{ClO_4}^-$
ν_{21}	634	0.30	635vs	$\delta_{\mathrm{OClO}}(66)$	$\nu_4\mathrm{ClO_4}^-+\delta(\phi)$
ν_{22}	674	0.00	747w	$\delta_{\mathrm{CCC}}(45)+\delta_{\mathrm{CCH}}(13)$	$\gamma(\phi)$
ν_{23}	728	0.35	826vs	$\Gamma_{\mathrm{CCCC}}(57)+\Gamma_{\mathrm{CCCH}}(20)$	$\delta(\phi)$
			847w		
ν_{24}	760	6.58	929m	$\nu_{\mathrm{OCl}}(98)$	$\nu_1\mathrm{ClO_4}^-$
ν_{25}	794	0.11	941w	$\nu_{\mathrm{NC}}(30)+\delta_{\mathrm{CCC}}(19)+\nu_{\mathrm{OC}}(14)$	ωC—H
ν_{26}	807	0.51	948m	$\Gamma_{\mathrm{CCCH}}(55)+\Gamma_{\mathrm{OCCH}}(17)+\Gamma_{\mathrm{NCCH}}(13)$	ωC—H
ν_{27}	829	0.94	954m	$\nu_{\mathrm{CC}}(56)+\nu_{\mathrm{OC}}(14)$	νC—C + νC—O
ν_{28}	831	24.80	1037vs	$\nu_{\mathrm{OCl}}(53)$	$\nu_3\mathrm{ClO_4}^-+\omega$C—H
ν_{29}	913	0.08		$\Gamma_{\mathrm{HCCH}}(40)+\Gamma_{\mathrm{CCCH}}(24)$	τC—H
ν_{30}	948	25.38	1013vs	$\nu_{\mathrm{OCl}}(90)$	$\nu_3\mathrm{ClO_4}^-$
ν_{31}	954	0.28		$\Gamma_{\mathrm{CCCH}}(64)+\Gamma_{\mathrm{NCCH}}(16)$	τC—H
ν_{32}	994	0.14		$\delta_{\mathrm{CCH}}(35)+\delta_{\mathrm{CCC}}(34)+\nu_{\mathrm{CC}}(32)$	νC—C + $\rho(\phi)$
ν_{33}	1040	0.77		$\delta_{\mathrm{CNH}}(31)+\nu_{\mathrm{OCl}}(28)+\Gamma_{\mathrm{CCNH}}(17)$	$\delta_{\mathrm{a}}\mathrm{NH_3}+\nu_3\mathrm{ClO_4}^-$, δN—H$\cdots$O
ν_{34}	1042	26.83	1087vs	$\nu_{\mathrm{OCl}}(37)+\delta_{\mathrm{CNH}}(22)$	$\nu_3\mathrm{ClO_4}^-+\delta_{\mathrm{a}}\mathrm{NH_3}$, δN—H$\cdots$O
ν_{35}	1051	8.81	1139vs	$\nu_{\mathrm{OCl}}(28)+\delta_{\mathrm{CNH}}(28)+\Gamma_{\mathrm{HNHO}}(21)+\nu_{\mathrm{CC}}(11)$	$\delta_{\mathrm{a}}\mathrm{NH_3}+\nu$C—C + $\nu_3\mathrm{ClO_4}^-$, δN—H$\cdots$O
ν_{36}	1108	1.09		$\delta_{\mathrm{CCH}}(55)+\nu_{\mathrm{CC}}(21)$	sciss C—H + νC—C
ν_{37}	1154	12.44		$\delta_{\mathrm{COH}}(58)+\nu_{\mathrm{CC}}(21)+\delta_{\mathrm{CCH}}(14)$	δO—H + νC—C + δC—H, δO—H$\cdots$O, 2.865 Å
ν_{38}	1168	1.41		$\delta_{\mathrm{CCH}}(70)+\nu_{\mathrm{CC}}(14)$	sciss C—H + νC—C
ν_{39}	1177	0.32		$\nu_{\mathrm{NC}}(41)+\nu_{\mathrm{CC}}(23)+\delta_{\mathrm{CCH}}(13)$	νC—N + νC—C + δC—H
ν_{40}	1254	8.93		$\nu_{\mathrm{OC}}(52)+\nu_{\mathrm{CC}}(22)$	νC—O + νC—C
ν_{41}	1314	0.06	1308w	$\nu_{\mathrm{CC}}(51)+\delta_{\mathrm{CCH}}(27)$	νC—C + ρC—H
ν_{42}	1328	2.64	1343m	$\delta_{\mathrm{CCH}}(45)+\nu_{\mathrm{CC}}(25)+\delta_{\mathrm{COH}}(20)$	νC—C + ρC—H + δO—H
			1363s		δO—H$\cdots$O, 2.865 Å
ν_{43}	1440	2.87	1440ssh	$\nu_{\mathrm{CC}}(33)+\delta_{\mathrm{CCH}}(24)$	νC—C + sciss C—H
ν_{44}	1497	17.75	1506vs	$\delta_{\mathrm{CCH}}(55)+\nu_{\mathrm{CC}}(27)$	νC—C + ρC—H
ν_{45}	1543	13.87	1516ssh	$\delta_{\mathrm{HNH}}(38)+\Gamma_{\mathrm{HNHO}}(35)+\delta_{\mathrm{CNH}}(30)$	$\delta_{\mathrm{s}}\mathrm{NH_3}$, δN—H$\cdots$O
ν_{46}	1567	1.95	1526s	$\delta_{\mathrm{HNH}}(50)+\delta_{\mathrm{CNH}}(18)+\Gamma_{\mathrm{CCNH}}(14)$	$\delta_{\mathrm{a}}\mathrm{NH_3}$, δN—H$\cdots$O
ν_{47}	1591	2.46	1592s	$\nu_{\mathrm{CC}}(53)+\delta_{\mathrm{HNH}}(10)$	νC—C + $\delta_{\mathrm{a}}\mathrm{NH_3}$, δN—H$\cdots$O
ν_{48}	1602	4.61	1609s	$\nu_{\mathrm{CC}}(64)+\delta_{\mathrm{CCH}}(16)$	νC—C
ν_{49}	1618	27.55	1627m	$\delta_{\mathrm{HNH}}(42)+\Gamma_{\mathrm{CCNH}}(24)+\nu_{\mathrm{CC}}(12)$	$\delta_{\mathrm{a}}\mathrm{NH_3}+\nu$C—C, δN—H$\cdots$O
ν_{50}	2830	11.09		$\nu_{\mathrm{NH}}(100)$	$\nu_{\mathrm{a}}\mathrm{NH_3}$, νN—H$\cdots$O
ν_{51}	2921	100	3106vs	$\nu_{\mathrm{NH}}(99)$	$\nu_{\mathrm{s}}\mathrm{NH_3}$, νN—H$\cdots$O
ν_{52}	3023	1.14		$\nu_{\mathrm{CH}}(98)$	νC—H aromatic
ν_{53}	3024	1.05		$\nu_{\mathrm{CH}}(99)$	νC—H aromatic
ν_{54}	3033	2.99	3037vs	$\nu_{\mathrm{CH}}(99)$	νC—H aromatic
ν_{55}	3062	0.03	3075vs	$\nu_{\mathrm{CH}}(96)$	νC—H aromatic
ν_{56}	3360	4.60	3179vs	$\nu_{\mathrm{NH}}(99)$	$\nu_{\mathrm{a}}\mathrm{NH_3}$, νN—H$\cdots$O
ν_{57}	3658	7.05	3490vs	$\nu_{\mathrm{OH}}(100)$	νO—H$\cdots$O, 2.865 Å

ν, stretching; a, antisymmetric; s, symmetric; δ, in-plane bending; γ, out-of-plane bending, ϕ, benzene ring; lib, librational; tor, torsional; τ, twisting; ω, wagging; ρ, rocking; sciss, scissoring.

[a] Obtained from the wave numbers calculated at B3LYP/6-311++G(d,p) using scaling factors 0.967 (for wave numbers under 1800 $\mathrm{cm^{-1}}$) and 0.955 (for those over 1800 $\mathrm{cm^{-1}}$).

[b] Relative absorption intensities normalized with highest peak absorption equal to 100.

[c] Total energy distribution calculated B3LYP/6-311++G(d,p) level of theory. Only contributions $\geq$10% are listed.

perchloric acid ($\nu_4 = 625\,\mathrm{cm^{-1}}$) are shown degenerate peaks. 539 $\mathrm{cm^{-1}}$, 544 $\mathrm{cm^{-1}}$ and 616 $\mathrm{cm^{-1}}$ peaks are assigned to the in-plane deformation peaks for 2HAP-$\mathrm{ClO_4}$ in FT-IR spectra. 537 $\mathrm{cm^{-1}}$, 549 $\mathrm{cm^{-1}}$ (555 $\mathrm{cm^{-1}}$), 569 $\mathrm{cm^{-1}}$ and 623 $\mathrm{cm^{-1}}$ (629 $\mathrm{cm^{-1}}$) peaks are determined as in-plane deformation vibrations for 3HAP-$\mathrm{ClO_4}$. In-plane deformation vibrations of 4HAP-$\mathrm{ClO_4}$ are observed at 625 $\mathrm{cm^{-1}}$ and 635 $\mathrm{cm^{-1}}$ in the FT-IR spectra. Symmetric stretching vibrations ($\nu_1 = 928\,\mathrm{cm^{-1}}$) of perchloric acid are observed at 757 $\mathrm{cm^{-1}}$ and 752 $\mathrm{cm^{-1}}$ (2HAP-$\mathrm{ClO_4}$), 939 $\mathrm{cm^{-1}}$ (3HAP-$\mathrm{ClO_4}$) and 929 $\mathrm{cm^{-1}}$ (4HAP-$\mathrm{ClO_4}$) in the FT-IR spectra. Out-of-plane deformations vibrations ($\nu_2 = 459\,\mathrm{cm^{-1}}$) of perchloric acid are observed at 417 $\mathrm{cm^{-1}}$ (2HAP-$\mathrm{ClO_4}$), 409 $\mathrm{cm^{-1}}$ (3HAP-$\mathrm{ClO_4}$) and 411 $\mathrm{cm^{-1}}$ (4HAP-$\mathrm{ClO_4}$) in the FT-IR spectra.

The non-hydrogen bonded or free hydroxyl group absorbs strongly in the 3700–3584 $\mathrm{cm^{-1}}$ region while the existence of intermolecular hydrogen bond formation can lower the O–H

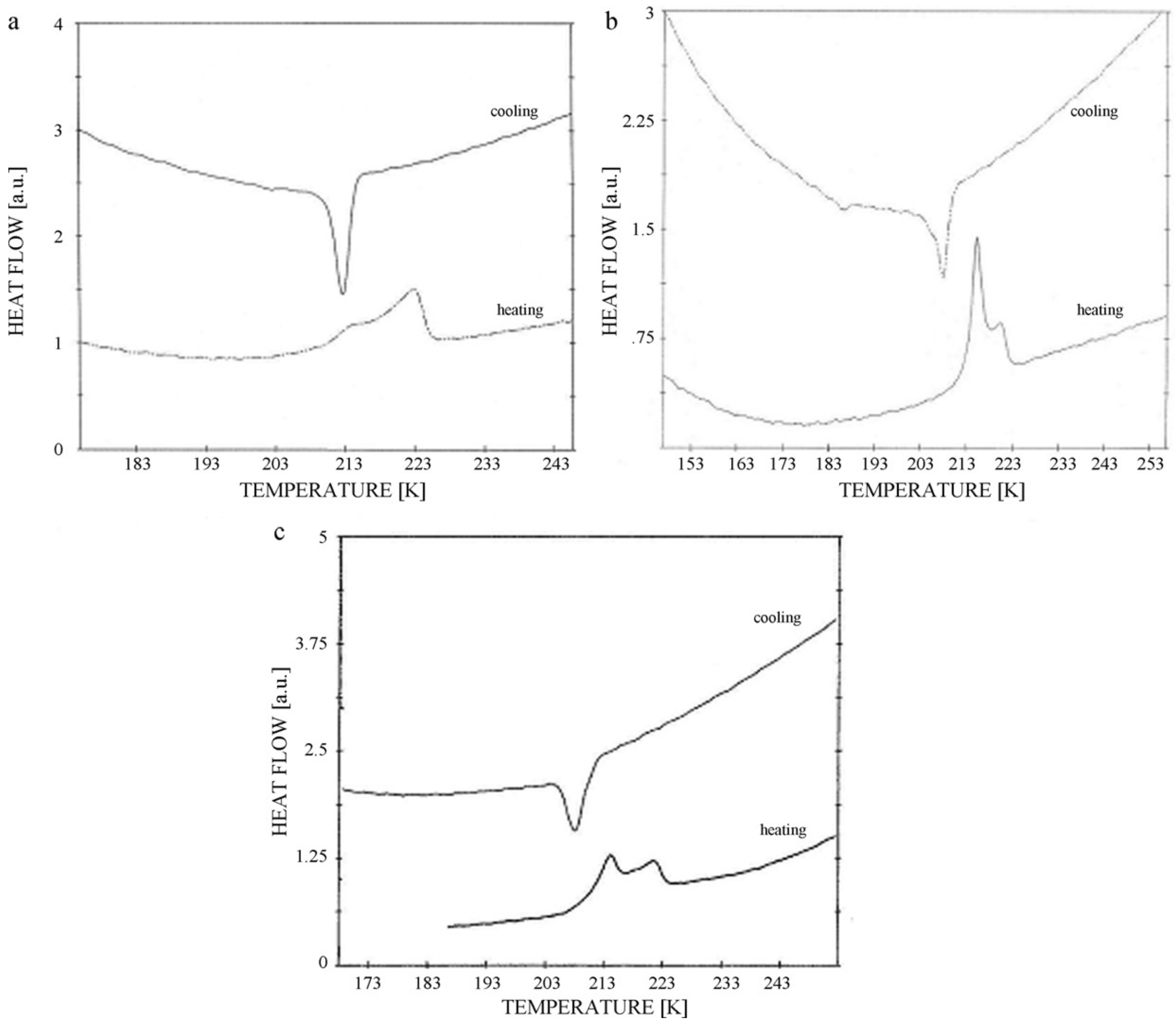

Fig. 3. DSC diagram for 2HAP-ClO_4 (a), 3HAP-ClO_4 (b) and 4HAP-ClO_4 (c) crystals.

stretching wavenumber to the 3550–3200 cm^{-1} region [21]. The band observed at 3441 cm^{-1} (2HAP-ClO_4), 3357 cm^{-1} (3HAP-ClO_4) and 3490 cm^{-1} (4HAP-ClO_4) vibrations are assigned to the O–H stretching vibrations. Theoretically computed frequencies were determined as 3669 cm^{-1}(2HAP-ClO_4), 3660 cm^{-1} (3HAP-ClO_4) and 3658 cm^{-1} (4HAP-ClO_4) by BLYP/6-311++G(d,p) method. This difference should be appeared, because experimental results belong to solid phase and theoretical calculations belong to gaseous phase. Moreover, the peak width, intensity and position of OH infrared bands are all affected by the extent of hydrogen bonding in a sample. The O–H stretching bands move to lower wavenumbers usually with increased intensity and band broadening in the hydrogen-bonded species [36].

The antisymmetric stretching vibration of aromatic primary amines was observed around 3500 cm^{-1}, while the symmetric one around 3400 cm^{-1} [22]. The theoretically computed values at 2839 cm^{-1} and 2927 cm^{-1} were assigned to the N–H stretching vibrations. 2839 cm^{-1} is assigned to the antisymmetric stretching vibration and observed at 2857 cm^{-1} in the FT-IR spectra. 2927 cm^{-1} peak is assigned to the symmetric stretching vibration and observed at 2924 cm^{-1} in the FT-IR spectra. The N–H stretching vibrations values in crystal environment are increasing, because of the hydrogen bonding effect through the perchloric acid. In the infrared spectrum, the bands observed at 1635 cm^{-1}, at 1630 cm^{-1}, at 1606 cm^{-1}, at 1594 cm^{-1} and 1574 cm^{-1} were assigned to antisymmetric bending vibrations of the NH_3 group of 2HAP-ClO_4. Symmetric bending vibrations of 2HAP-ClO_4 are observed at 1522 cm^{-1}, at 1515 cm^{-1} and 1510 cm^{-1} in the FT-IR spectra. These peaks are observed at 1617 cm^{-1} (antisymmetric), at 1580 cm^{-1} (antisymmetric), at 1540 cm^{-1} (antisymmetric), at 1503 cm^{-1} (symmetric) for 3HAP-ClO_4. Three bands observed at 1627 cm^{-1}, and 1592 cm^{-1} and 1526 cm^{-1} in the infrared spectrum were assigned to antisymmetric NH_3 bending vibrations. Symmetric bending vibration is observed at 1516 cm^{-1} in the FT-IR spectra.

The bands occur in the region 3000–3010 cm^{-1} and are strong to medium intensity is due to the aromatic C–H stretching wavenumbers [23]. In the 2HAP-ClO_4 compound, the strong band in FT-IR at 3016 cm^{-1}, 3030 cm^{-1}, 3049 cm^{-1} and 3067 cm^{-1} is assigned for C–H stretching wavenumber. The CH stretching vibrations are observed at 3053 cm^{-1} and 3064 cm^{-1} (3HAP-ClO_4), 3037 cm^{-1} and 3075 cm^{-1} (4HAP-ClO_4) in the FT-IR spectra. The calculated corresponding values fall the same region. In the high frequency region, the TED calculations show that all the C–H stretching vibrations are pure modes.

4.4. *Differential scanning calorimetry (DSC)*

The DSC curves for 2-hydroxyanilinium perchlorate, 3-hydroxyanilinium perchlorate and 4-hydroxyanilinium perchlorate crystals recorded upon heating and cooling are displayed in

Table 6
Values of energetic effect for observed phase transitions.

	2-Hydroxyanilinium perchlorate	3-Hydroxyanilinium perchlorate	4-Hydroxyanilinium perchlorate
Heating			
Peak from [K]	205.76	210.41	208.31
Peak to [K]	226.23	222.87	224.17
Onset [K]	214.97	213.26	212.07
Peak [K]	222.94	215.27	214.10
J/g	1.07	0.98	1.11
Sample weight [mg]	11.514	11.921	2.424
Scanning rate [K/min]	20	20	20
Cooling			
Peak from [K]	207.81	199.77	206.92
Peak to [K]	215.89	211.73	216.70
Onset [K]	214.45	209.77	209.37
Peak [K]	212.77	207.95	213.63
J/g	−0.72	−0.57	−0.84
Sample weight [mg]	11.514	11.921	2.424
Scanning rate [K/min]	20	20	20

Fig. 3. All three crystals demonstrate analogous behavior. Performed measurements revealed that they undergo fully reversible and discontinuous phase transitions at similar temperatures (close to 215 K), see Table 6 for details. Taking into account the value of energetic effect (*ca.* 1 J/g) these phase transitions should be regarded as “order–disorder” type. It is worthwhile mentioning here that on DSC runs registered during cooling of the samples, only one peak is observed, while for heating, two components are clearly visible. It is suggested that mechanism of observed phase transitions, being similar for each studied crystal, is complex and is likely two step process.

4.5. HOMO, LUMO analysis

The atomic orbital compositions of the frontier molecular orbitals of 2, 3 and 4-hydroxyanilinium perchlorate are shown in Fig. 4. The HOMO–LUMO energy gap of these compounds was calculated at the B3LYP/6-311++(d,p) level. The HOMO represents the ability to donate an electron, LUMO as an electron acceptor represents the ability to obtain an electron.

According to the Koopman theorem, the energies of LUMO and HOMO can be described to a good approximation as [24]:

$$\chi \cong -\frac{1}{2}(E_{\mathrm{HOMO}} + E_{\mathrm{LUMO}}) \tag{1}$$

$$\eta \cong -\frac{1}{2}(E_{\mathrm{HOMO}} - E_{\mathrm{LUMO}}) \tag{2}$$

Several important molecular properties such as chemical hardness (η) and electronegativity (χ) have been defined based on density functional theory [25–27]. Chemical hardness has been used as a tool to understand the chemical reactivity and some other properties of a molecular system [28]. It has also been shown that stability of molecules is related to its chemical hardness [29]. The concept of electronegativity has been introduced as the power of an atom in a molecule to attract electrons onto itself [30]. Chemical hardness (η), and electronegativity (χ) are defined in Eqs. (1) and (2). As a result, when the gap is large (other things being equal), one expects high stability and low reactivity. When it is small, one expects low stability and high reactivity [31].

The low value of HOMO–LUMO gap 5.767 eV (Fig. 4) in 3-hydroxyanilinium perchlorate while comparing to 2-hydroxyanilinium perchlorate (5.867 eV) and 4-hydroxyanilinium perchlorate (5.865 eV) reflects the chemically reactive nature. The decrease in the HOMO and LUMO energy gap explains the eventual charge transfer interaction taking place within the molecule which is responsible for the activity of the molecule. Consequently, the lowering of the HOMO–LUMO band gap is essentially a consequence of the large stabilization of the LUMO due to the strong electron-acceptor ability of the electron-acceptor group.

4.6. Molecular electrostatic potential

The molecular electrostatic potential (MESP) is the most useful electrostatic property to study the relation between structure and activity. The MESP has been also employed as an informative tool of chemistry to describe different physical and chemical features, including non-covalent interactions in complex biological system.

The electrostatic potential created by the nuclei and electrons of a molecule in the surrounding space is well established as a guide to the interpretation and prediction of molecular behavior. It has been shown to be a useful tool in studying both electrophilic and nucleophilic processes, in particular, to be well suited for studies that involve the identification of key features necessary for the “recognition” of one molecule by another. The molecular surface electrostatic potential (MSEP) is rigorously defined as the first order interaction between a positive unit charge at any point in the vicinity of a molecule and its charge distribution contributed by both electrons and nuclei. The potential $V(r)$ can be calculated through Eq. (3)

$$V(r) = \sum_{A} \frac{Z_A}{|R_A - r|} = \int \frac{\rho(r')dr'}{r' - r} \tag{3}$$

where Z_A is the charge on nucleus A; at a distance R_A; and $\rho(r)$ is the electronic density function defined by the 0.001 a.u. contour.

The electron density isosurface on to which the electrostatic potential surface has been mapped is shown in Fig. 5 for 2, 3 and 4-hydroxyanilinium perchlorate compounds. The different values of the electrostatic potential at the surface are represented by different colors; red represents regions of most negative electrostatic potential, blue represents regions of most positive electrostatic potential and green represents regions of zero potential.

It is seen in Fig. 5 that 2, 3 and 4-hydroxyanilinium perchlorate compounds have almost similar isosurfaces. A negative energy region (red color) is located over the perchloric acid. The positive energy area (blue color) is observed over the NH_3 group of aminophenol ring. The red regions refer to an area that would favor interactions with approaching electrophiles. $V(r)$ minima are in lone pair region in a plane bisecting the H–N–H angle predicting a site of hydrogen bonding acceptors. The blue regions interact extensively with incoming nucleophiles and thus the sites of hydrogen bond donor groups [32–35].

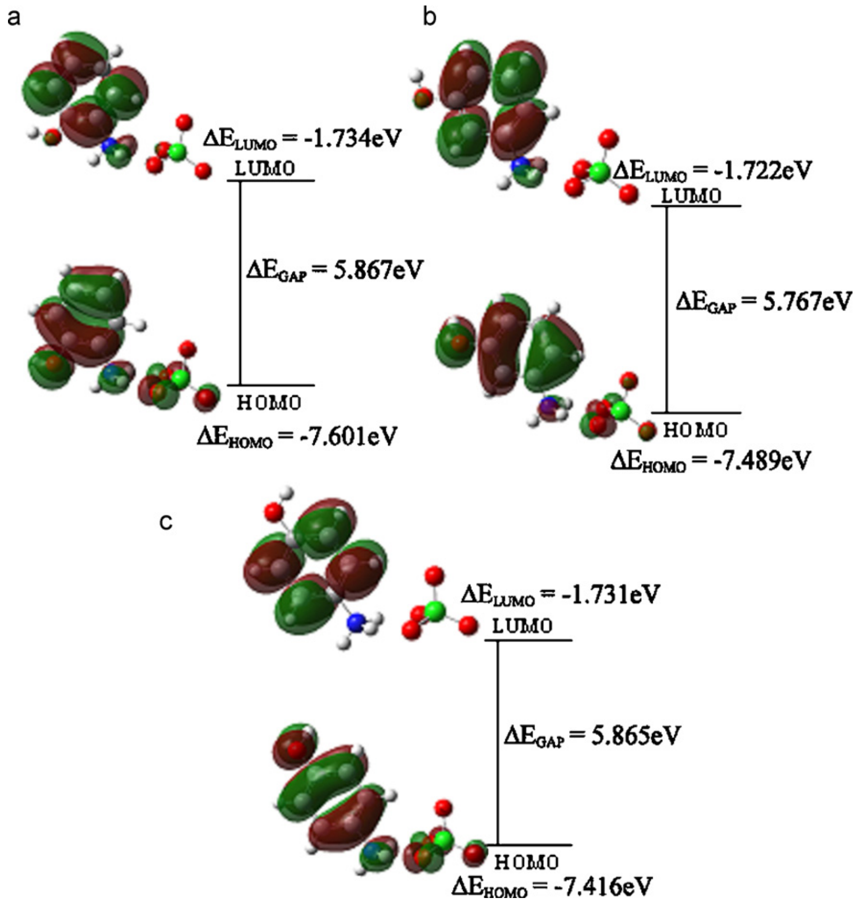

Fig. 4. HOMO–LUMO plots of 2-hydroxyanilinium perchlorate (a), 3-hydroxyanilinium perchlorate (b) and 4-hydroxyanilinium perchlorate (c) compounds.

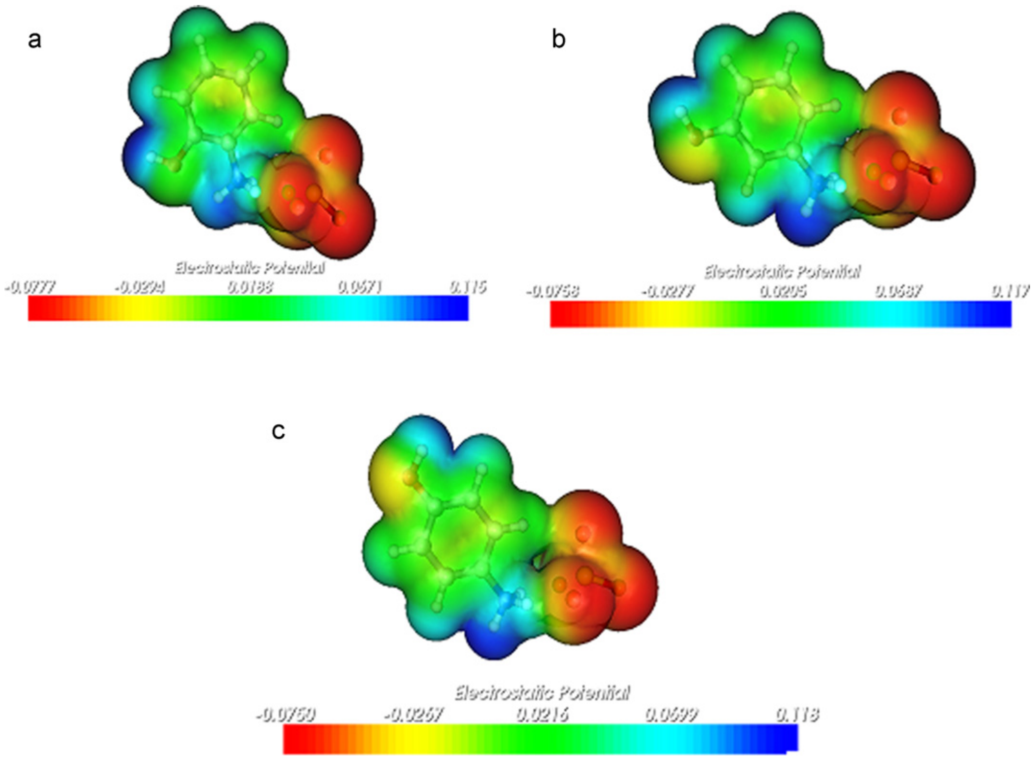

Fig. 5. B3LYP/6-311++G(d,p) calculated 3D molecular electrostatic potential of 2-hydroxyanilinium perchlorate (a), 3-hydroxyanilinium perchlorate (b) and 4-hydroxyanilinium perchlorate (c) compounds. (For interpretation of the references to color in this figure legend, the reader is referred to the web version of the article.)

5. Conclusion

Recently reported complexes of perchloric acid (with 2-hydroxyaniline, 3-hydroxyaniline and 4-hydroxyaniline) were investigated in details. The energies, geometric parameters and vibrational frequencies for the title compounds were calculated using B3LYP with 6-311++G(d,p) basis set. Comparison between the calculated geometric parameters and the X-ray structure show good agreement. The calculated frequencies were scaled with 0.967 and 0.955 for wavenumbers under 1800 cm^{-1} and over 1800 cm^{-1}, respectively.

Characteristic bands originating from vibrations of perchloric anions and hydroxyanilinium cations are assigned taking into account the results of TED calculations with additional help of visual inspections (MOLDEN). Comparison between the vibrational wavenumbers obtained in this manner, and the measured FT-IR spectra shows that they are in good agreement and support each other. The influence of intermolecular interactions (hydrogen bonds) on differences between experimental (solid phase) and theoretical (gaseous phase) frequencies are noticed and explained. On the basis of differential scanning calorimetric (DSC) measurements it is suggested that mechanism of observed phase transitions, being similar for each studied crystal, is complex and is likely two step process.

The decrease in the HOMO and LUMO energy gap explains the eventual charge transfer interaction taking place within the molecule which is responsible for the NLO activity. It is worthwhile to mention here that the X-ray structures for two of the studied crystals (3-hydroxyaniline with perchloric acid and 4-hydroxyaniline with perchloric acid [18]) were solved in non-centrosymmetric space groups ($P2_1$ and $P2_12_12_1$, respectively). Appropriate regions related to electrophilic and nucleophilic reactivity were determined and depicted for the studied compounds on the basis of molecular electrostatic potential (MESP) calculations.

Acknowledgement

The author (Y. Erdogdu) would like to thank Ahi Evran University Research Fund for its financial support. The work was financially supported by National Science Centre (Project No. N N507 2218 40).

References

[1] M. Szafran, A. Katrusiak, Z. Dega-Szafran, J. Mol. Struct. 880 (2008) 77–85.
[2] S.B. Monaco, L.E. Davis, S.P. Velsko, F.T. Wang, D. Eimerl, A. Zalkin, J. Cryst. Growth 85 (1987) 252–255.
[3] A.M. Petrosyan, Vib. Spectrosc. 41 (2006) 97–100.
[4] M.K. Marchewka, unpublished data.
[5] P. Teulon, R.G. Delaplane, I. Olovsson, Acta Crystallogr. C 41 (1985) 479–483.
[6] M. Stammler, R. Bruenner, W. Schmidt, D. Orcutt, Adv. X-ray Anal. 9 (1966) 170–189.
[7] M. Mylrajan, T.K.K. Srinivasan, J. Raman Spectrosc. 22 (1991) 53–55.
[8] P. Czarnecki, W. Nawrocik, Z. Pająk, J. Wąsicki, Phys. Rev. B 49 (1994) 1511–1512.
[9] P. Czarnecki, W. Nawrocik, Z. Pająk, J. Wąsicki, J. Phys. Condens. Matter 6 (1994) 4955.
[10] P. Czarnecki, J. Wąsicki, Z. Pająk, R. Goc, H. Małuszyńska, S. Habryło, J. Mol. Struct. 404 (1997) 175–180.
[11] M.K. Marchewka, M. Drozd, A. Pietraszko, Mat. Sci. Eng. B 100 (2003) 225–233.
[12] E. Grech, Z. Malarski, L. Sobczyk, J. Potier, J. Rozière, J. Mol. Struct. 178 (1988) 23–28.
[13] M. Ji, M. Odelius, K.J. Gaffney, Science 328 (2010) 1003–1005.
[14] M.J. Frisch, G.W. Trucks, H.B. Schlegel, G.E. Scuseria, M.A. Robb, J.R. Cheeseman, G. Scalmani, V. Barone, B. Mennucci, G.A. Petersson, H. Nakatsuji, M. Caricato, X. Li, H.P. Hratchian, A.F. Izmaylov, J. Bloino, G. Zheng, J.L. Sonnenberg, M. Hada, M. Ehara, K. Toyota, R. Fukuda, J. Hasegawa, M. Ishida, T. Nakajima, Y. Honda, O. Kitao, H. Nakai, T. Vreven, J.A. Montgomery, J.E. Peralta Jr., F. Ogliaro, M. Bearpark, J.J. Heyd, E. Brothers, K.N. Kudin, V.N. Staroverov, R. Kobayashi, J. Normand, K. Raghavachari, A. Rendell, J.C. Burant, S.S. Iyengar, J. Tomasi, M. Cossi, N. Rega, J.M. Millam, M. Klene, J.E. Knox, J.B. Cross, V. Bakken, C. Adamo, J. Jaramillo, R. Gomperts, R.E. Stratmann, O. Yazyev, A.J. Austin, R. Cammi, C. Pomelli, J.W. Ochterski, R.L. Martin, K. Morokuma, V.G. Zakrzewski, G.A. Voth, P. Salvador, J.J. Dannenberg, S. Dapprich, A.D. Daniels, O. Farkas, J.B. Foresman, J.V. Ortiz, J. Cioslowski, D.J. Fox, Gaussian 09, Revision A.02, Gaussian, Inc., Wallingford, CT, 2009.
[15] G. Rauhut, P. Pulay, J. Phys. Chem. 99 (1995) 3093–3100.
[16] Y. Erdogdu, O. Unsalan, M.T. Gulluoglu, J. Raman Spectrosc. 41 (7) (2010) 820–828.
[17] Y. Erdogdu, O. Unsalan, M. Amalanathan, I. Hubert Joe, J. Mol. Struct. 980 (2010) 24–30.
[18] J. Janczak, G.J. Perpetuo, Solid State Sci. 11 (2009) 1576–1581.
[19] H. Siebert, Z. Anorg, Allg. Chem. 275 (1954) 225–240.
[20] M. Ilczyszyn, D. Godzisz, M.M. Ilczyszyn, J. Mol. Struct. 611 (2002) 103–118.
[21] D. Sajan, Y. Erdogdu, T. Kuruvilla, I.H. Joe, J. Mol. Struct. 983 (2010) 12–21.
[22] V. Krishnakumar, N. Prabavathi, J. Raman Spectrosc. 39 (2008) 679–684.
[23] H. Saleem, A.R. Krishnan, Y. Erdogdu, S. Subashchandrabose, V. Thanikachalam, G. Manikandan, J. Mol. Struct. 999 (2011) 2–9.
[24] X.-P. Chen, Y.-Q. Ding, Q.-W. Teng, Chin. J. Chem. Phys. 21 (2008) 105–110.
[25] R.G. Parr, R.A. Donnelly, M. Levy, W.E. Palke, J. Chem. Phys. 68 (1978) 3801.
[26] R.G. Parr, R.G. Pearson, J. Am. Chem. Soc. 105 (1983) 7512–7516.
[27] R.G. Parr, L.V. Szentpaly, S. Liu, J. Am. Chem. Soc. 121 (1999) 1922–1924.
[28] R.G. Parr, P.K. Chattaraj, J. Am. Chem. Soc. 113 (1991) 1854–1855.
[29] Z. Zhou, R.G. Parr, J. Am. Chem. Soc. 112 (1990) 5720–5724.
[30] L. Pauling, The Nature of the Chemical Bond, 3rd ed., Cornell University Press, 1967.
[31] W. Kohn, A.D. Becke, R.G. Parr, J. Phys. Chem. 100 (1996) 12974–12980.
[32] I. Fleming, Frontier Orbitals and Organic Chemical Reactions, John Wiley and Sons, New York, 1976.
[33] J.S. Murray, K. Sen, Molecular Electrostatic Potentials, Concepts and Applications, Elsevier, Amsterdam, 1996.
[34] J.M. Seminario, Recent Developments and Applications of Modern Density Functional Theory, vol. 4, Elsevier, 1999, pp. 800–806.
[35] T. Yesilkaynak, G. Binzet, F. Mehmet Emen, U. Florke, N. Kulcu, H. Arslan, Eur. J. Chem. 1 (2010) 1–5.
[36] A. Novak, Hydrogen bonding in solids. Correlation of spectroscopic and crystallographic data, in: J.D. Dunitz, P. Hemmerich, R.H. Holm, J.A. Ibers, C.K. Jørgensen, J.B. Neilands, D. Reinen, R.J.P. Williams (Eds.), Structure and Bonding, vol. 18, Springer, Heidelberg, 1974.